



TALLINN UNIVERSITY OF TECHNOLOGY
SCHOOL OF ENGINEERING
Department of Civil Engineering and Architecture

ANALYSIS OF FIRE DESIGN MODELS OF THE NEW EUROCODE 5 FOR I-SHAPED MEMBERS

UUE EUROKODEKS 5 JÄRGSE I-KUJULISTE PUIDUST ELEMENTIDE TULEPÜSIVUSE PROJEKTEERIMISMUDELI ANALÜÜS

MASTER THESIS

Üliõpilane: Greete Sulg

Üliõpilaskood: 177522EAEI

Juhendaja: Prof. Alar Just

Tallinn 2023

Lihtlitsents lõputöö reprodutseerimiseks ja lõputöö üldsusele kättesaadavaks tegemiseks¹

Mina, Greete Sulg,

1. Annan Tallinna Tehnikaülikoolile tasuta loa (lihtlitsentsi) enda loodud teose "Uue Eurokoodeks 5 järgse I-kujuliste puidust elementide tulepüsivuse projekteerimismudeli analüüs", mille juhendaja on Alar Just,

1.1 reprodutseerimiseks lõputöö säilitamise ja elektroonse avaldamise eesmärgil, sh Tallinna Tehnikaülikooli raamatukogu digikogusse lisamise eesmärgil kuni autoriõiguse kehtivuse tähtaja lõppemiseni;

1.2 üldsusele kättesaadavaks tegemiseks Tallinna Tehnikaülikooli veebikeskkonna kaudu, sealhulgas Tallinna Tehnikaülikooli raamatukogu digikogu kaudu kuni autoriõiguse kehtivuse tähtaja lõppemiseni.

2. olen teadlik, et käesoleva lihtlitsentsi punktis 1 nimetatud õigused jäävad alles ka autorile.

3. kinnitan, et lihtlitsentsi andmisega ei rikuta teiste isikute intellektuaalomandi ega isikuandmete kaitse seadusest ning muudest õigusaktidest tulenevaid õigusi.

¹Lihtlitsents ei kehti juurdepääsupiirangu kehtivuse ajal, välja arvatud ülikooli õigus lõputööd reprodutseerida üksnes säilitamise eesmärgil.

_____ (allkiri)

_____ (kuupäev)

Department of Civil Engineering and Architecture

THESIS TASK

Student: Greete Sulg, 177522EAEI
Study programme: EAEI02/17 Structural Engineering and Construction Management
Supervisor(s): Professor Alar Just

Thesis topic: Analysis of fire design models of the new Eurocode 5 for I-shaped members

Uue Eurokoodeks 5 järgse I-kujuliste puidust elementide tulepüsivuse projekteerimismudeli analüüs

Thesis main objectives:

1. Calculations according to the new Eurocode 5 Part 1-2:2025 (Annex I)
2. Comparison between calculations (EN1995:2025) and test results
3. Propositions for the new Eurocode 5 Part 1-2:2025 calculation method

Thesis tasks and time schedule:

No	Task description	Deadline
1.	Creating calculation tables with formulas from EN1995-1-2:2025	
2.	Analysis of the tests	
3.	Comparison of test results and calculation method	
4.	Formalization	

Language: english **Deadline for submission of thesis:** 22.05.2023

Student: Greete Sulg
/signature/

Supervisor: Alar Just
/signature/

CONTENTS

List of abbreviations and symbols	7
1. INTRODUCTION.....	10
2. I-SHAPED MEMBERS	12
2.1 Introduction of wooden I-shaped members.....	12
2.2 Fire	13
2.2.1 Standard fire	13
2.2.2 The European charring model	14
3. CALCULATION FROM THE GUIDELINE "FIRE SAFETY IN TIMBER BUILDINGS"	17
3.1 Presumptions for calculation	17
3.2 Charring depth	18
3.3 Reduced properties method	19
3.3.1 Strength parameters	19
3.4 Reduced cross-section method	22
3.4.1 Zero-strength layer thickness d_0	22
3.4.2 Strength parameters	23
4. CALCULATION ACCORDING TO EN 1995-1-2:2025	25
4.1 Presumptions for calculation	25
4.1.1 Protection level of an insulation material	25
4.1.2 Duration of the charring phases	27
4.2 Formulas for calculating floors	28
4.2.1 Calculation for the flange on the fire exposed side	28
4.2.2 Calculation for flange on the lateral side.....	31
4.2.3 Calculation for the web	33
4.2.4 Strength parameters	34
4.3 Formulas for calculating walls	34
4.3.1 Zero-strength layer thickness d_0	34
4.3.2 Stiffness and wall buckling	35
4.3.3 Buckling out of walls plane (around y-axle)	35
4.3.4 Buckling in walls plane, around z-axle.....	36
4.3.5 Strength parameters	38
5. FIRE TESTS.....	39
5.1 Full-scale floor test	39
5.2 Full-scale wall test.....	41
6. COMPARISON OF TEST RESULTS AND CALCULATIONS (EN 1995-1-2:2025)	45
6.1 Floors	45
6.1.1 Comparison between failure times t_f	45

6.1.2 Load bearing capacity	47
6.2 Walls	53
6.2.1 Comparison between failure times t_f	53
6.2.2 Load bearing capacity	56
6.3 Conclusions	61
7. PROPOSITIONS FOR EUROCODE 5 PART 1-2:2025.....	63
SUMMARY	66
KOKKUVÕTE	68
REFERENCES	70

List of abbreviations and symbols

Latin upper case letters

E_w	Mean value of the modulus of elasticity of the web
E_f	Mean value of the modulus of elasticity of the flange
I_{ef}	Effective moment of inertia of the cross-section
I_f	Contribution of the remaining flanges to the moment on inertia
I_w	Contribution of the remaining web to the moment of inertia
E_{web}	Modulus of elasticity of the web
$L_{z,ef}$	Buckling length of the I-joist in wall plane
M_k	Characteristic bending resistance
W_{ef}	Section modulus of the cross-section

Latin lower case letters

b_f, b	Initial cross-section width of the flange
$b_{f,ef}$	Effective cross-section width of the flange
b_w	Initial cross-section width of the web
$b_{w,ef}$	Effective cross-section width of the web
d_0	Zero-strength layer depth
$d_{char,n}$	Notional charring depth within one charring phase
$d_{char,n,1}$	Notional charring depth at fire exposed side
$d_{char,n,2}$	Notional charring depth at lateral side
$d_{char,n,w}$	Notional charring depth of the web
d_{ef}	Effective charring depth
$f_{c,0,k}$	Compressive strength along the grain
$f_{m,0,k}$	Bending strength
$f_{t,0,k}$	Tensile strength
f_{20}	20% fractile of the bending strength
h	Initial cross-section depth of the I-joist
h_f	Initial cross-section depth of the flange

$h_{f,ef}$	Effective cross-section depth of the flange
h_{ins}	Minimum thickness of the cavity insulation
h_p	Panel thickness
h_w	Cross-section depth of the web
k	Web stiffness
k_w	Factor for reduction of buckling length
k_0	Zero-strength layer coefficient
k_2	Protection factor for Phase 2
$k_{3,1}$	Post-protection factor for the fire exposed side
$k_{3,2}$	Post-protection factor for lateral side
k_4	Consolidation factor for Phase 4
k_h	Thickness factor
$k_{s,n,1}$	Combined section and conversion factor for the fire exposed side
$k_{s,n,2}$	Combined section and conversion factor for the lateral side
k_ρ	Density factor
t	Time of fire exposure, time for the charring phase considered
t_a	Consolidation time
t_{ch}	Start time of charring on the fire exposed side
$t_{ch,2}$	Start time of charring on the lateral side
$t_{ch,w}$	Start time of charring of the web
t_f	Failure time of panels initially exposed to fire
$t_{f,pr}$	Failure time of the fire protection system
$t_{prot,i}$	Protection time of the layer i with thickness h_i

Greek upper-case letters

Σt_{prot}	Sum of protection times
$\Sigma t_{prot,i}$	Sum of the protection times of the layers i
$\Sigma t_{prot,i-1}$	Sum of the protection times of the layers preceding the layer i

Greek lower-case letters

β_0	Basic design charring rate
β_n	Notional charring rate within one charring phase
$\beta_{n,Phase2}$	Notional design charring rate during Phase 2
$\beta_{n,Phase3}$	Notional design charring rate during Phase 3
γ_M	Partial factor for the relevant mechanical material property
$\gamma_{M,fi}$	Partial factor for the relevant mechanical material property for fire
ρ_k	Characteristic density

1. INTRODUCTION

In the current era, it is important to create sustainable and eco-friendly buildings. Using renewable materials in construction is a way to achieve efficient building solutions. One material that has gained significant attention in recent years is wood. Using timber as primary construction material does not compromise on performance, load bearing capacities or acoustic properties.

Incorporation of wood in constructions can be accomplished through the use of I-shaped wooden members in timber frame assemblies. I-joists can serve as load-bearing construction elements, as they hold superior strength-to-weight ratios compared to steel. Additionally, the flanges and web of I-joists can be jointed together, allowing for the creation of longer spans that would otherwise be impractical with sawn timber. [1]

I-joists are typically manufactured using strength graded timber or laminated veneer lumber (LVL) for the flanges and oriented strand board (OSB) or plywood for the web. To ensure consistent and reliable performance, I-shaped members are constructed under strict quality control conditions - low moisture content during production minimizes the effects of shrinking.

Historically, the primary reason for avoiding wooden elements in building construction was due to fire safety requirements. With advancements in technology, timber can now be efficiently protected using different protection systems, resulting in a significant increase in its usage. Constructions containing I-shaped members are more sensitive to the fire as they tend to burn more quickly due to the smaller parameters of the cross-section. Therefore, it is essential to understand how I-shaped members perform in fire to ensure that the engineers have reliable guidelines when designing safer buildings.

Currently, there is no standardized method to calculate I-shaped elements in fire situations. The only available approach for design of I-shaped elements is outlined in the Guideline "Fire Safety in Timber Buildings". However, this method has considerable limitations that restrict its suitability for common cases, such as void cavity and wall calculations. Previous research has examined the behavior of I-joists in fire situations, with the aim of creating efficient equations for designing I-shaped cross-sections.

With the development of the new formulas specifically for I-shaped cross-sections in the new Eurocode 5 Part 1-2:2025, it becomes important to evaluate effectiveness of the calculation method. This thesis inspects deeper into the calculation method, aiming to identify any potential errors that may arise during the element design. Given the

complexity of the equations involved, it is crucial that engineers have a thorough understanding of the equations and values used.

Aim of the thesis

The aim of this thesis is to test the calculation method for I-shaped members provided in Annex I of EN 1995-1-2:2025 in the future and to find potential challenges from the user perspective. The other aim was to compare calculation results with the full scale fire test results.

In addition to above, this thesis proposes improvements to Eurocode 5 Part 1-2:2025 Annex I to simplify the calculation process and provide additional explanations and figures to better describe the calculation methodology.

The body of this thesis is structured into three main parts. The first part assesses the currently available calculation method for I-joists, providing a description of the method through a calculation example. The second part gives a detailed description of the calculation method outlined in Annex I of the EN 1995-1-2:2025, presented in the same order as the calculation should be carried out. Finally, the third part demonstrates the test results and compares them to the results received from the calculation method.

Keywords: wooden I-joist, fire resistance, Eurocode 5

2. I-SHAPED MEMBERS

2.1 Introduction of wooden I-shaped members

I-shaped elements are considered to be composite members. Strength graded structural timber or LVL is primarily used to construct the flanges and the web consists of particle board or OSB. These three components along with timber joints are bonded together using resin-based adhesive. I-joists are made from carefully selected timber and board material which makes them 44% stronger than steel in proportion to weight. [1]



Figure 2.1-1 I-shaped elements

Initially, the houses were typically constructed using solid lumber beams and columns, resulting in a significant amount of wood being wasted. However, with the introduction of I-joists, the amount of waste is considerably reduced. The use of wooden materials in web construction is beneficial since it is from timber that would otherwise be unused. As a result, less raw material is required compared to traditional wooden frames.

I-joists are most commonly used as load-bearing elements in timber frame assemblies, which are used for constructing walls, floors or roofs. The wooden elements are typically covered on both sides with gypsum or OSB boards. These assemblies can be manufactured either on-site or in a factory. Two cavity options are available: either leave them void or fill them with insulation. [2]

The I-shaped product ensures the effective load transfer through the whole cross-section, achieving great strength properties relative to the amount of material used. The flanges contribute to bending strength and stiffness, while the web provides shear resistance. Nevertheless, it is important to take into consideration the webs buckling

and flanges splitting. The combination of different materials and the slender nature of I-joists makes their fire resistance a complicated issue. [1]

Since the I-joists are sensitive to fire exposure, they must be effectively protected against fire. In the case of protected cross-sections, the start time of charring is delayed. In addition to that, char layer is protecting the cross-section even more. After the failure of the claddings, the charring is influenced by cavity insulation. This also helps to protect it and hold off the start time of charring on the lateral side. [3]

Using protective materials with timber beams has a positive effect in fire situations. Covering the beam with for example gypsum board, delays start time of charring. Gypsum board provides good fire protection because it consists of about 20% water that keeps temperatures at 100°C for a certain period of time in case of fire. When the protection layer remains in place after start time of charring, the rate of charring slowed down.

The calculation method for wooden I-joists in EN 1995-1-2:2025 Annex I is based on the model for timber member assemblies with I-joists by Mäger (2019, 2020) and with rectangular cross-sections by Tiso (2018). However, due to the smaller cross-sectional area of the flanges, the thin web, and the presence of adhesives, I-joists are more vulnerable to elevated temperatures than rectangular cross-sections. This results in more complex calculations. [1]

2.2 Fire

2.2.1 Standard fire

To ensure a standardized fire exposure, various time-temperature curves are available for use. In pr EN 1991-1-2, the standard fire exposure is defined by the time-temperature curve presented in Figure 2.2.1-1. In the present thesis the standard fire curve is used in all tests and calculations.

In fire situation when the temperature exceeds 300°C timber and wood-based panels exposed to fire start to char. This also occurs behind the protection system, as the temperatures are high. Already at 100°C the water start evaporating and this is a beginning for charring process. [3]

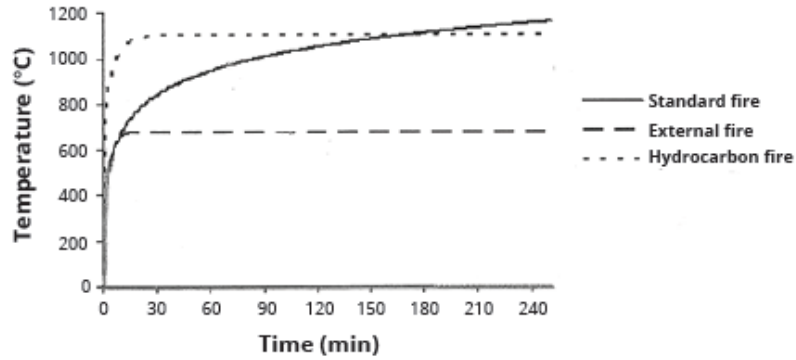


Figure 2.2.1-1 Nominal temperature-time curves given in EN 1991-1-2

The capacity of load-bearing structural timber members that are exposed to fire can be affected by a variety of factors, including material properties, geometrical characteristics, protection, and thermal boundary conditions. [4]

2.2.2 The European charring model

The updated EN 1995-1-2:2025 incorporates a new approach of categorizing charring into different phases. The division takes into account the presence and duration of the fire protection system. This should be applied to standard fire exposure. [5]

- | | |
|---|--|
| Phase 1 – normal charring phase | - Initially protected sides of timber member or initially unprotected sides of timber member |
| Phase 0 – encapsulated phase | - No charring occurs behind the protection system |
| Phase 2 – protected charring phase | - Charring occurs behind the protection system while the system is still in place |
| Phase 3 – post-protected charring phase | - After the failure of the protection system before a fully developed char layer has been formed |
| Phase 4 – consolidated charring phase | - Fully developed char layer and consolidated charring rate |

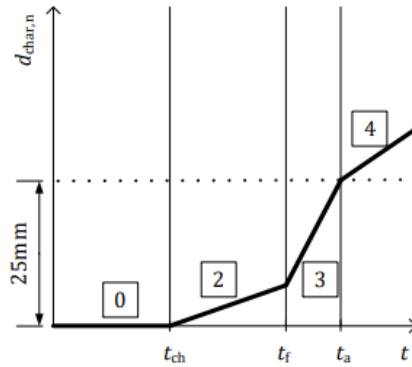


Figure 2.2.2-1 European Charring Model for initially protected timber member [6]

Each phase is defined by a specific time period that represents the characteristic events occurring during that phase. In Phase 0, there is no evidence of charring. Phase 2 is comparatively slow, with the protection system still intact. However, once the protective layer fails, charring in Phase 3 becomes rapid. Once a consolidated char layer forms, Phase 4 shows a reduction in the rate of charring. [6]

Timber members exposed to fire exhibit charring unless they are protected during the relevant time of fire exposure. According to EN 1995-1-2:2025 the notional charring depth of a timber member $d_{char,n}$ can be calculated with formula 5.1 [5]

$$d_{char,n} = \sum_{phases} (\beta_n t) \tag{5.1}$$

- where
- $d_{char,n}$ - notional charring depth, mm
 - β_n - notional design charring rate within one charring phase, mm/min
 - t - time for the charring phase considered, min

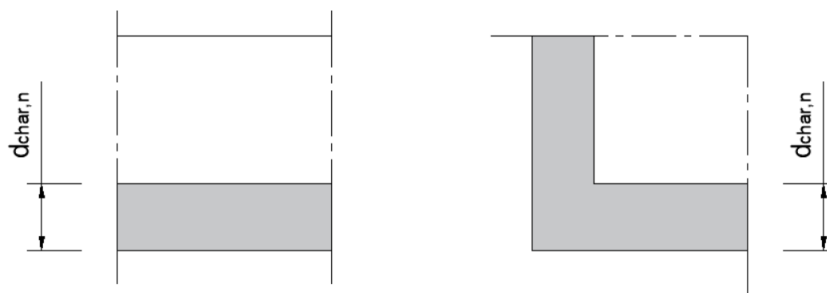


Figure 2.2.2-2 Notional charring depth $d_{char,n}$

The start time of charring is primarily defined by the material characteristics of the protective layer and the backing material. The formula used in this thesis assumes that the fire protection system contains gypsum boards.

$$t_{ch} = \min \left\{ \begin{array}{l} \sum t_{prot} \\ t_{f,pr} \end{array} \right. \quad (5.7)$$

where

t_{ch}	-	start time of charring behind the protection system, min
$\sum t_{prot}$	-	sum of protection times of the fire protection system, min
$t_{f,pr}$	-	failure time of the protection system, min

The fall of time of protective layers t_f depends on the cladding material, the fastening system, the backing material and the orientation. Research and tests have shown that fall off time of the protection system is shortest when backed by insulation materials and longer when backed by massive timber or void cavities. [6]

According to the new EN 1995-1-2:2025 Table 6.1 and Table 6.2, it is possible to easily evaluate failure time of the protection system. If needed to be more precise there are formulas to calculate the failure times t_f within Table 5.5.

This thesis uses panels specified in Table 5.5 of EN 1995-1-2:2025 as the protection system. The failure time of the protection system $t_{f,pr}$ should be calculated as follows

$$t_{f,pr} = t_f \quad (5.9)$$

where

t_f	-	failure time of the protection system, min
-------	---	--

3. CALCULATION FROM THE GUIDELINE "FIRE SAFETY IN TIMBER BUILDINGS"

3.1 Presumptions for calculation

This chapter describes the calculation technique used to evaluate floor assemblies with lightweight I-joists in fire situation. Currently, this is the only method available to determine the performance of I-joists during a fire. The method is outlined in the European Technical Guideline "Fire Safety in Timber Buildings". [3]

This calculation distinguishes between two charring phases to indicate the time when the protection system falls off.

Charring phase 2 - the failure of assembly take place at or before the time of failure of protection system

Charring phase 3 - the failure of assembly take place after the time of failure of protection system t_f

where t_f - failure time of the protection system, min

There are two methods available in the European standards for calculating the strength parameters in fire situation. The first method, known as reduced cross-section method (or effective cross-section method) is using the original cross-section which is reduced by effective charring depth d_{ef} . The second method, known as the reduced properties method, which reduces the cross-section by $d_{char,n}$ and also modifies the factors related to fire. [3]

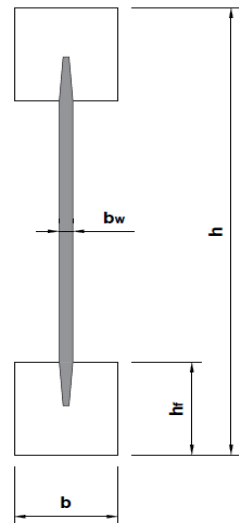
Guideline "Fire Safety in Timber Buildings" presents a calculation method for evaluating bending members, which is applicable to I-joists of floor assemblies. However, it's important to note that this method is only considered valid if the I-joists are situated within timber frame assemblies that are either fully or partially insulated.

Below an example calculation is given with the parameters selected by author, which are listed in Table 3.1-1 on the next page.

All the equations are numbered according to Guideline "Fire Safety in Timber Buildings".

Table 3.1-1 Timber frame assembly parameters for the calculation

Cross-section			
Height of the I-joist	h	200	mm
Width of the flanges	b	47	mm
Height of the flanges	h _f	47	mm
Width of the web	b _w	10	mm
Materials			
Wood strength class for flanges		C30	
One dimensional charring rate	β ₀	0,65	mm/min
		OSB	
Width of the web		<13	mm
Protective layers			
Gypsum board type F 15mm	t _{ch}	20	min
	t _f	22,5	min
Glass wool insulation	h _{ins}	200	mm
Fire information			
Duration of fire	t	30	min



3.2 Charring depth

The first step in the calculation process is to determine the notional charring depth, which differs for charring phase 2 and charring phase 3.

The notional charring rate β_n for charring phase 2 is calculated as

$$\beta_n = \beta_0 k_{b,ch} k_2 k_n = 0,65 * 1,58 * 1 * 1,4 = 1,44 \text{ mm/min} \quad (6.85)$$

$$k_{b,ch} = \frac{27,4}{b} + 1 = \frac{27,4}{47} + 1 = 1,58 \quad (6.81)$$

- where
- β₀ - one dimensional charring rate, mm/min
 - k_{b,ch} - coefficient
 - k₂ - coefficient, k₂ = 1
 - k_n - coefficient, k_n = 1,4
 - b - width of the flange, mm

For charring phase 2, d_{char,n} is calculated as

$$d_{char,n} = \beta_n(t - t_{ch}) = 1,44 * (30 - 20) = 14,4 \text{ mm} \quad (6.84)$$

- where
- d_{char,n} - notional charring depth, mm
 - β_n - notional charring rate, mm/min

- t - time of fire exposure, min
- t_{ch} - start time of charring, min

The notional charring rate β_n for charring phase 3 is calculated as

$$\beta_n = \beta_0 k_{b,ch} k_3 k_n = 0,65 * 1,58 * 1,35 * 1,4 = 1,95 \text{ mm/min} \quad (6.80)$$

$$k_3 = 0,0157 t_f + 1 = 0,0157 * 22,5 + 1 = 1,35 \quad (6.82)$$

- where
- β_0 - one dimensional charring rate, mm/min
 - k_3 - coefficient
 - k_n - coefficient, $k_n = 1,4$

For charring phase 3, $d_{char,n}$ is calculated as

$$d_{char,n} = \beta_n (t - t_{f,ef}) = 1,95 * (30 - 20,25) = 19,0 \text{ mm} \quad (6.79)$$

$$t_{f,ef} = 0,9 t_f = 0,9 * 22,5 = 20,25 \text{ min} \quad (6.83)$$

- where
- $t_{f,ef}$ - effective failure time of the protection system, min
 - t_f - failure time of the protection system, min

3.3 Reduced properties method

This method allows to calculate the charring depth for phase 2 or phase 3, described above. In order to calculate strength parameters during fire, there are formulas that adjust the parameters for the fire. The modification factors also take into account the strength of finger joints depending on adhesive.

3.3.1 Strength parameters

Since the calculation method presented focuses on calculating bending strength, it should be noted that the flange on fire exposed side takes on tensile strength while the other flange is in compression. In order to calculate modification factor, is it necessary to first determine following factors

$$k_{b,fm} = 0,76 + \frac{11,5}{b} = 0,76 + \frac{11,5}{47} = 1,01 \quad (6.87)$$

$$k_{hf,fm} = \frac{68}{h_f} - 0,41 = \frac{68}{47} - 0,41 = 1,04 \quad (6.88)$$

$$k_{h,fm} = 1,4 - \frac{80}{h} = 1,4 - \frac{80}{200} = 1,0 \quad (6.89)$$

The failure in this case takes place in Charring Phase 2, then $k_{mod,fi}$ should be calculated as

$$k_{mod,fi} = 1 - 0,016 d_{char,n} k_{b,fm} k_{hf,fm} k_{h,fm} = \quad (6.86)$$

$$= 1 - 0,016 * 14,41 * 1,01 * 1,04 * 1,0 = 0,76$$

where $d_{char,n}$ - notional charring depth, mm
 b - width of the flange, mm
 h_f - depth of the flange, mm
 h - cross-section height, mm

Bending resistance for I-joist is calculated taking bending strength $f_{m,k}$ of the fire exposed flange. Since the mean flange design stresses $\sigma_{f,c,d}$ and $\sigma_{f,t,d}$ should not be greater than the design compressive and tensile strength of the flanges, $f_{m,k}$ can be replaced with

$$f_{m,k,ef} = \min \left\{ \begin{array}{l} \frac{f_{c,k} h}{h - h_f} \\ \frac{f_{t,k} h}{h - h_f} \end{array} \right. = \min \left\{ \begin{array}{l} \frac{23 * 181}{181 - 47} = 31,07 \\ \frac{18 * 181}{181 - 28} = 21,29 \end{array} \right. = 21,29 \text{ N/mm}^2 \quad (6.78)$$

It's important to note that, in this formula, the parameters are based on the remaining cross-section after the effects of charring have been taken into account.

Finger-joint strength is dependent on the adhesive used. Since I-joists are prone to finger-joint failures in the tension flanges, this should be taken in consideration while calculating. Design value for bending resistance $f_{m,d,fi}$ should be calculated as

$$f_{m,d,fi} = k_{mod,fi} k_{mod,fi} k_{fi} \frac{f_k}{\gamma_{M,fi}} = 0,76 * 1 * 1,25 * \frac{21,29}{1} = 20,23 \text{ N/mm}^2 \quad (6.93)$$

- where
- $f_{m,d,fi}$ - bending strength in fire situation, N/mm²
 - $k_{mod,fi}$ - modification factor for fire
 - $k_{mod,fj,fi}$ - modification factor for finger joints in fire
 - k_{fi} - modification factor for a strength property for the fire situation
 - f_k - bending strength of the flange, N/mm²
 - $\gamma_{M,fi}$ - partial safety factor for timber in fire

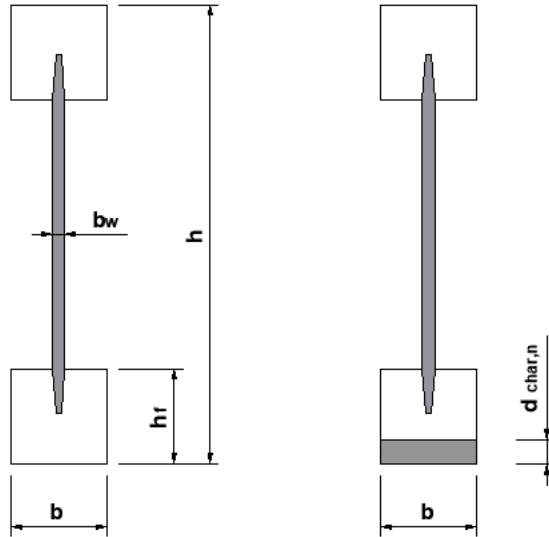


Figure 3.3.1-1 Cross-section of I-joist, at ambient conditions and in the fire situation

To calculate characteristic bending resistance, section modulus W_{ef} and effective moment of inertia of the cross section I_{ef} is needed. Those can be calculated as

$$W_{ef} = \frac{2 I_{ef}}{h} = \frac{2 * 17,65 * 10^6}{181} = 19,61 * 10^4 \text{ mm}^3 \quad (6.76)$$

$$I_{ef} = I_f + \frac{E_w}{E_f} I_w = 17,47 * 10^6 + \frac{2200}{12000} * 0,99 * 10^6 = 17,65 * 10^6 \text{ mm}^4 \quad (6.77)$$

- where
- E_f - mean value of the modulus of elasticity of the flange, MPa
 - E_w - mean value of the modulus of elasticity of the web, MPa
 - I_f - contribution of the remaining flanges to the moment on inertia, mm⁴
 - I_w - contribution of the remaining web to the moment of inertia, mm⁴

The moment on inertia values are calculated using the parameters of the remaining cross-section.

With those parameters it is possible to calculate the characteristic bending resistance M_k .

$$M_k = f_{m,k} W_{ef} k_h = 21,29 * 19,61 * 10^4 * 1,0 = 4,17 \text{ kNm} \quad (6.75)$$

where $f_{m,k}$ - characteristic bending strength of the I-joist
 k_h - depth effect, where applicable

3.4 Reduced cross-section method

According to the reduced cross-section method, the reduction of strength and stiffness parameters are considered by assuming normal temperature properties of timber multiplied by k_{fi} . However, zero-strength layer depth d_0 is subtracted from the residual cross-section. Charring of the cross-section is calculated as shown in Chapter 3.2.

3.4.1 Zero-strength layer thickness d_0

The zero-strength layer is a fictive layer that compensates for the strength loss at elevated temperatures. [7] For I-joists zero-strength layer thickness should be calculated as

$$d_0 = 5,3 + 0,165h_f - 0,018b - 0,0006h_f b = \quad (6.94)$$

$$= 5,3 + 0,165 * 47 - 0,018 * 47 - 0,0006 * 47 * 47 = 10,9 \text{ mm}$$

where h_f - height of the flange on the fire exposed side, mm
 b - width of the flange on the fire exposed side, mm

In calculations the cross-section is reduced by d_{ef} , which is calculated as

$$d_{ef} = d_{char,n} + k_0 d_0 = 14,4 + 1,0 * 10,9 = 25,3 \text{ mm} \quad (6.23)$$

where d_{ef} - effective charring depth, mm
 k_0 - zero-strength layer coefficient
 d_0 - zero-strength layer thickness, mm

$$k_0 = \begin{cases} \frac{t}{20} \leq 1 \rightarrow \frac{t}{t_{ch}} = \frac{30}{20} = 1,5 \rightarrow 1 & \text{for unprotected members} \\ \frac{t}{t_{ch}} & \text{for protected members} \end{cases} \quad (6.24)$$

3.4.2 Strength parameters

Since the limited zone immediately below the char-line of the residual cross-section is heated above normal temperature, strength in this zone is reduced.

Bending strength for fire situation should be calculated as

$$f_{m,d,fi} = k_{mod,fi} \frac{f_{20}}{\gamma_{M,fi}} = 1,0 * \frac{1,25 * 30}{1,0} = 37,5 \text{ N/mm}^2 \quad (6.17)$$

- where
- f_{20} - 20% fractile of the bending strength, N/mm²
 - $k_{mod,fi}$ - modification factor for fire expressing the reduction of strength
 - $\gamma_{M,fi}$ - partial safety factor for timber in fire

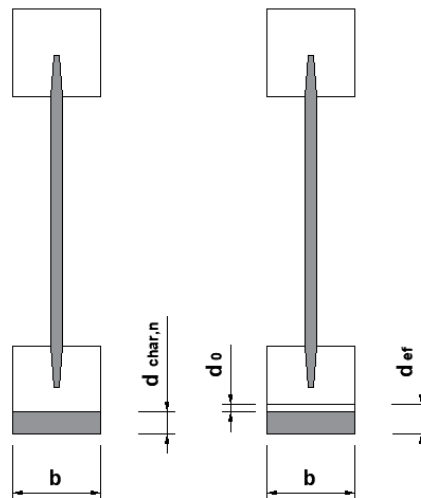


Figure 3.4.2-1 Notional charring depth $d_{char,n}$, zero-strength layer d_0 and effective charring depth d_{ef}

The maximum bending moment of the I-joist is calculated using the formulas described earlier

$$W_{ef} = \frac{2 I_{ef}}{h} = \frac{2 * 0,63 * 10^6}{174,71} = 0,72 * 10^4 \text{ mm}^3 \quad (6.76)$$

$$I_{ef} = I_f + \frac{E_w}{E_f} I_w = 0,45 * 10^6 + \frac{2200}{12000} * 0,99 * 10^6 = 0,63 * 10^6 \text{ mm}^4 \quad (6.77)$$

$$M_k = f_{m,k} W_{ef} k_h = 30 * 0,72 * 10^4 * 1,0 = \mathbf{2,77 \text{ kNm}} \quad (6.75)$$

The moment of inertia values are calculated using the parameters of the remaining cross-section.

The calculation described in this chapter presumes the knowledge about the charring phase during which the I-joist failure occurs. The results of these two calculations differ by approximately 30%

4. CALCULATION ACCORDING TO EN 1995-1-2:2025

4.1 Presumptions for calculation

The fire design calculation for I-joists is proposed in Annex I of the future design standard EN 1995-1-2:2025. This chapter describes a calculation method for timber frame assemblies with I-shaped cross-sections and a panel at least on one side. This thesis gives an overview for fully insulated cavities with PL1 and PL2 insulation and void cavities.

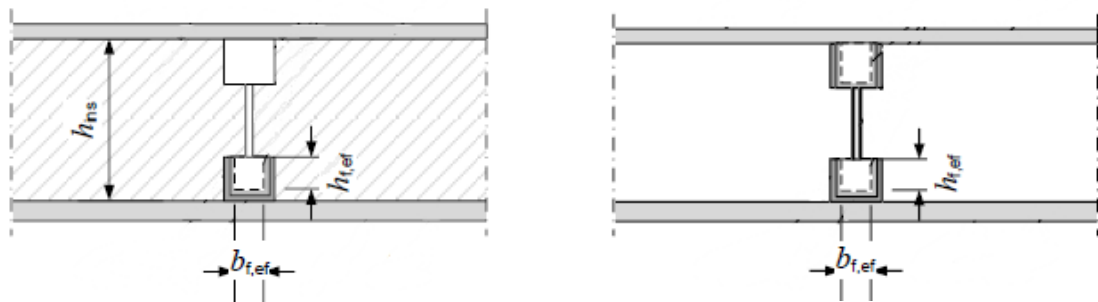


Figure 4.1-1 Fully insulated cavity, void cavity

4.1.1 Protection level of an insulation material

In timber frame assemblies, cavities are typically filled with insulation to protect the lateral sides of the studs or joists. However, despite the presence of insulation, charring can still occur on the lateral side of the cross-section.

EN 1995-1-2:2025 categorizes insulation into three groups based on its effectiveness in protecting the lateral sides of timber members. Insulation materials are divided into groups according to their protective ability to reduce charring on the lateral sides of timber member. [4]

Protection level 1	-	Provides the best protection and the charring from the lateral sides of the cross section is reduced	Stone wool
Protection level 2	-	Provides some protection and the charring on the lateral side starts but the protection disappears due to recession	Glass wool, wood fiber, cellulose fiber

- Protection level 3 - Provides almost no protection and the charring on the lateral side can start before failure of the fire protection system. XPS, EPS, PUR, PIR, etc.

As the insulation with the parameters for PL3 is not recommended for the I-joists, this will not be covered in this thesis.

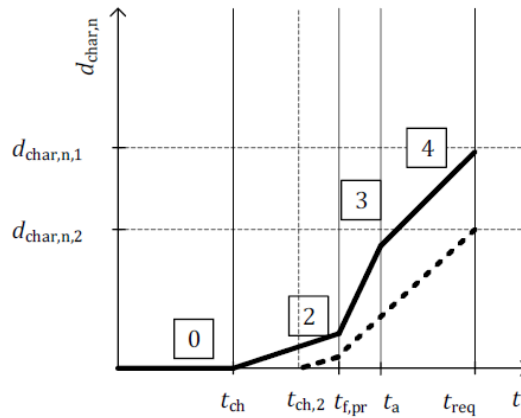


Figure 4.1.1-1 Charring phases with cavity insulations PL1 and PL2 when $t_{ch,2} \leq t_{f,pr}$

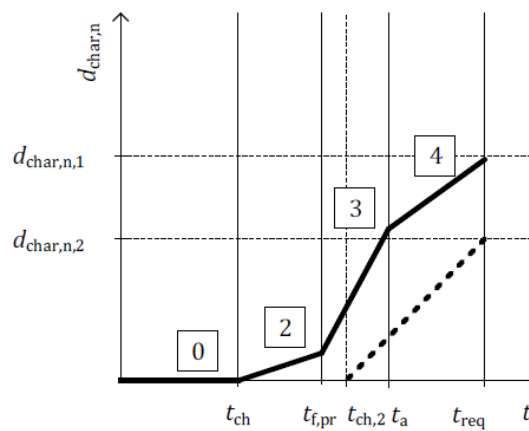


Figure 4.1.1-2 Charring phases with cavity insulation PL1 and PL2 when $t_{ch,2} > t_{f,pr}$

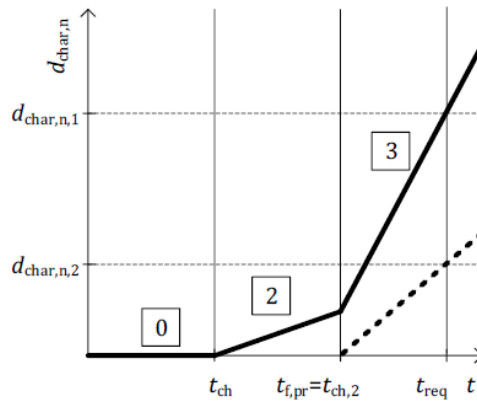


Figure 4.1.1-3 Charring phases for void cavities

4.1.2 Duration of the charring phases

Phase 1, which describes initially unprotected sides of timber members, is not relevant to the calculation being discussed in this thesis.

Phase 0 describes a phase when charring is prevented due to the effect of fire protection system.

Phase 2 begins at the start time of charring t_{ch} and continues until the protection system fails $t_{f,pr}$. However, it should be noted that the start time of charring for lateral sides of the I-joist sides is calculated differently.

The start time of charring for the flange on the fire-exposed side is dependent on the failure time of the protection system.

$$t_{ch} = \min \left\{ \begin{array}{l} \sum t_{prot} \\ t_{f,pr} \end{array} \right. \quad \begin{array}{l} \text{for fire protection system consisting other} \\ \text{than timber and wood-based materials} \end{array} \quad (5.7)$$

For flange, start time of charring on the lateral side is calculated as

$$t_{ch,2} = \sum t_{prot,i-1} + t_{prot,i} \quad \begin{array}{l} \text{for cavity insulation PL1 and PL2} \\ \text{for void cavities} \end{array} \quad (I.27)$$

$$t_{ch,2} = t_{f,pr} \quad (I.12)$$

The initial charring on the lateral side of a timber member can occur in phase 2, 3, or 4, depending on the insulation and protection system used.

For the web, start time of charring on the lateral side is calculated as

$$t_{ch,w} = \sum t_{prot,i-1} + t_{prot,i} \quad \text{for cavity insulation PL1 and PL2} \quad (I.28)$$

After the failure of the protection system, the I-joist and cavity insulation will be directly exposed to fire.

Phase 3 describes the fast charring which lasts for a short time. It occurs from failure time of the protection system $t_{f,pr}$ until the consolidation time t_a which is calculated as

$$t_a = 1,04 t_{f,pr} \quad \text{for PL1} \quad (I.25)$$

$$t_a = 1,01 t_{f,pr} \quad \text{for PL2} \quad (I.26)$$

Phase 4 occurs after the consolidation time t_a , which means that it exists when the fire exposure time t is greater than t_a . In other words Phase 4 represents the time period between t_a and t .

4.2 Formulas for calculating floors

This calculation method applies to timber member assemblies with I-joists used in floors, where at least one side of the I-shaped cross-section is protected with a fire protection system.

Gypsum board is used as the protection system for the I-joists in this calculation method. Failure time t_f of the panels initially exposed to fire is taken from the Table 5.5 from EN 1995-1-2:2025.

4.2.1 Calculation for the flange on the fire exposed side

The notional charring rates of the I-joists flange on the fire exposed should be calculated as

$$\beta_n = k_2 k_{s,n,1} \beta_o \quad \text{for phase 2} \quad (I.10)$$

$$\beta_n = k_{3,1} k_{s,n,1} \beta_o \quad \text{for phase 3} \quad (I.12)$$

$$\beta_n = k_4 k_{s,n,1} \beta_o \quad \text{for phase 4} \quad (I.14)$$

with

$$k_{s,n,1} = 9,48 b_f^{-0,43} \quad \text{for PL1} \quad (\text{I.15})$$

$$k_{s,n,1} = 6,39 b_f^{-0,36} \quad \text{for PL2 or void cavity} \quad (\text{I.17})$$

The Annex I of the EN 1995-1-2:2025 does not provide the $k_{s,n,1}$ factor for void cavities. In this case, it is appropriate to consider it as PL2. This selection is based on two factors: the dependence of the factor on the flange width (b_f), and the fact that the value should be greater than 1. Additionally, choosing PL2 for void cavities is justified because the behavior of insulation closely resembles that of void cavities.

- where
- β_n - notional design charring rate within one charring phase, mm/min
 - k_2 - protection factor for phase 2
 - $k_{s,n,1}$ - combined conversion and section factor for the fire exposed side
 - β_o - basic design charring rate, mm/min
 - $k_{3,1}$ - post-protection factor for phase 3 for the fire exposed side
 - k_4 - factor for phase 4
 - b_f - initial cross-section width of the flange, mm

Calculation of factors is performed based on the following formulas

$$k_2 = 1 - \frac{h_p}{55} \quad \text{for gypsum plasterboards} \quad (\text{5.3})$$

$$k_{3,1} = 6,5 - \frac{t_{f,pr}}{25} \quad \text{for PL1} \quad (\text{I.19})$$

$$k_{3,1} = 20 - 0,22 t_{f,pr} \quad \text{for PL2} \quad (\text{I.21})$$

$$k_{3,1} = 2 \quad \text{for void cavities}$$

$$k_4 = 0,9 + \frac{t_a}{48} \quad \text{for PL1} \quad (\text{I.23})$$

$$k_4 = 3,7 + \frac{t_a}{48} \quad \text{for PL2} \quad (\text{I.24})$$

- where
- h_p - thickness of the panel(s) of the same material, mm
 - $t_{f,pr}$ - failure time of the protection system, min
 - t_a - consolidation time, min

Notional charring depth $d_{char,n,1}$ for the fire exposed side is calculated using notional charring rates β_n for each respective charring phase.

$$d_{char,n,1} = \sum_{phases} (\beta_n t) \quad (I.7)$$

Once the charring depth is determined, the next step is to calculate the thickness of the zero-strength layer d_0 . This factor is calculated by taking into account the strength of the finger joints. For timber frame assemblies with PL1 insulation, d_0 should be calculated as

$$d_0 = \max \left\{ \begin{array}{l} \frac{t_{f,pr}}{70} d_{char,n,1} - \frac{t_{f,pr}}{2200} d_{char,n,1}^2 + 1,6 \ln(b_f) - 1 \\ 1,6 \ln(b_f) - 1 \end{array} \right. \quad \begin{array}{l} \text{for finger joint class} \\ 1 \text{ (FJ1) or without} \\ \text{joints} \end{array} \quad (I.32)$$

$$d_0 = \max \left\{ \begin{array}{l} \frac{t_{f,pr}}{70} d_{char,n,1} - \frac{t_{f,pr}}{2200} d_{char,n,1}^2 + 1,6 \ln(b_f) + 1 \\ 1,6 \ln(b_f) + 1 \end{array} \right. \quad \begin{array}{l} \text{for finger joint class} \\ 2 \text{ (FJ2)} \end{array} \quad (I.33)$$

$$d_0 = \max \left\{ \begin{array}{l} \frac{t_{f,pr}}{70} d_{char,n,1} - \frac{t_{f,pr}}{2200} d_{char,n,1}^2 + 1,6 \ln(b_f) + 3 \\ 1,6 \ln(b_f) + 3 \end{array} \right. \quad \begin{array}{l} \text{for finger joint class} \\ 3 \text{ (FJ3)} \end{array} \quad (I.34)$$

For timber frame assemblies with PL2 insulation or void cavities, d_0 should be calculated as

$$d_0 = \max \left\{ \begin{array}{l} \frac{t_{f,pr}}{74} d_{char,n,1} - \frac{t_{f,pr}}{2700} d_{char,n,1}^2 + 1,6 \ln(b_f) - 1,4 \\ 1,6 \ln(b_f) - 1,4 \end{array} \right. \quad \begin{array}{l} \text{for finger joint class} \\ 1 \text{ (FJ1) or without} \\ \text{joints} \end{array} \quad (I.32)$$

$$d_0 = \max \left\{ \begin{array}{l} \frac{t_{f,pr}}{74} d_{char,n,1} - \frac{t_{f,pr}}{2700} d_{char,n,1}^2 + 1,6 \ln(b_f) + 0,6 \\ 1,6 \ln(b_f) + 0,6 \end{array} \right. \quad \begin{array}{l} \text{for finger joint class} \\ 2 \text{ (FJ2)} \end{array} \quad (I.33)$$

$$d_0 = \max \left\{ \begin{array}{l} \frac{t_{f,pr}}{74} d_{char,n,1} - \frac{t_{f,pr}}{2700} d_{char,n,1}^2 + 1,6 \ln(b_f) + 1,6 \\ 1,6 \ln(b_f) + 1,6 \end{array} \right. \quad \begin{array}{l} \text{for finger joint class} \\ 3 \text{ (FJ3)} \end{array} \quad (I.34)$$

If the fire exposure time t is less than the failure time of the fire protection system $t_{f,pr}$ then the fire exposure time t should be used.

The effective cross-section depth of the flange can be calculated using the following formulas

$$h_{f,ef} = h_f - d_{ef} \quad (I.2)$$

$$d_{ef} = d_{char,n,1} + d_0 \quad (I.3)$$

- where
- $h_{f,ef}$ - effective cross-section depth of the flange, mm
 - h_f - initial cross-section depth of the flange, mm
 - d_{ef} - effective charring depth, mm
 - $d_{char,n,1}$ - notional charring depth at the fire exposed side, mm
 - d_0 - zero-strength layer thickness, mm

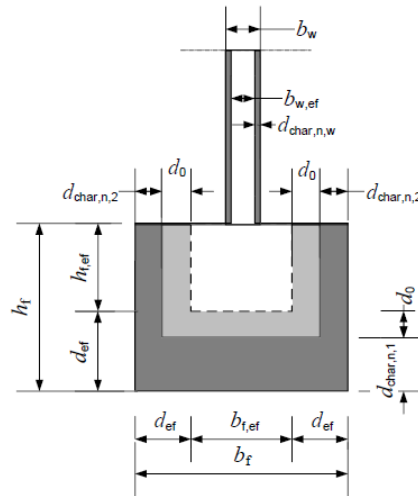


Figure 4.2.1-1 Flange on the fire exposed side

4.2.2 Calculation for flange on the lateral side

The notional charring rates of the I-joists flange on the lateral side should be calculated as

$$\beta_n = k_2 k_{s,n,2} \beta_0 \quad \text{for phase 2} \quad (I.11)$$

$$\beta_n = k_{3,2} k_{s,n,2} \beta_0 \quad \text{for phase 3} \quad (I.13)$$

with

$$k_{s,n,2} = 2,25 h_f^{-0,13} \quad \text{for PL1} \quad (I.16)$$

$$k_{s,n,2} = 6,39 h_f^{-0,18} \quad \text{for PL2 or void cavity} \quad (I.18)$$

where $k_{s,n,2}$ - combined conversion and section factor for the lateral side
 $k_{3,2}$ - post-protection factor for phase 3 for the lateral side
 h_f - initial cross-section depth of the flange, mm

Calculation of factors is performed based on the following formulas

$$k_2 = 1 - \frac{h_p}{55} \quad \text{for gypsum plasterboards} \quad (5.3)$$

$$k_{3,2} = 0,01 + \frac{\max(t_{f,pr}; t_{ch,2})}{338} \quad \text{for PL1} \quad (I.20)$$

$$k_{3,2} = 0,03 + \frac{\max(t_{f,pr}; t_{ch,2})}{338} \quad \text{for PL2} \quad (I.22)$$

$$k_{3,1} = 2 \quad \text{for void cavities}$$

where h_p - thickness of the panel(s) of the same material, mm
 $t_{f,pr}$ - failure time of the protection system, min
 $t_{ch,2}$ - start time of charring for the lateral side, min

With notional charring rate β_n it is now possible to calculate notional charring depth $d_{char,n,2}$ for the lateral side

$$d_{char,n,2} = \sum_{phases} (\beta_n t) \quad (I.7)$$

Once the charring depth is determined, the next step is to calculate the thickness of the zero-strength layer d_0 . This factor is calculated by taking into account the strength of the finger joints. Formulas for this calculation are described in Chapter 4.2.1.

The effective cross-section width of the flange should be calculated as

$$b_{f,ef} = b_f - 2 d_{ef} \quad (I.2)$$

$$d_{ef} = d_{char,n,2} + d_0 \quad (I.3)$$

where $b_{f,ef}$ - effective cross-section width of the flange, mm
 b_f - initial cross-section width of the flange, mm
 d_{ef} - effective charring depth, mm
 $d_{char,n,2}$ - notional charring depth at the lateral side, mm
 d_0 - zero-strength layer thickness, mm

4.2.3 Calculation for the web

The notional charring rates of the web of the I-joist can be calculated as

$$\beta_n = k_2 k_{s,n,2} \beta_o \quad \text{for phase 2} \quad (\text{I.11})$$

$$\beta_n = k_{3,2} k_{s,n,2} \beta_o \quad \text{for phase 3} \quad (\text{I.13})$$

with

$$k_{s,n,2} = 1$$

- where
- $k_{s,n,2}$ - combined conversion and section factor for the lateral side
 - $k_{3,2}$ - post-protection factor for phase 3 for the lateral side
 - h_f - initial cross-section depth of the flange, mm

For the basic design charring rate for OSB β_0 , the material density and thickness must be considered. It is calculated as follows

$$\beta_0 = \prod k_i * \beta_o = k_h * k_\rho * \beta_o \quad (\text{5.2})$$

- where
- $\prod k_i$ - product of applicable modification factors for charring k_i
 - k_h - thickness factor
 - k_ρ - density factor

Factors are calculated according to

$$k_2 = 1 - \frac{h_p}{55} \quad \text{for gypsum plasterboards} \quad (\text{5.3})$$

$$k_{3,2} = 2$$

- where h_p - thickness of the panel(s) of the same material, mm

With notional charring rate β_n , it is now possible to calculate notional charring depth $d_{char,n,w}$ for the lateral side of the web

$$d_{char,n,w} = \sum_{phases} (\beta_n t) \quad (\text{I.9})$$

The effective cross-section width of the web should be calculated as

$$b_{w,ef} = b_w - 2 d_{char,n,w} \quad (I.6)$$

where

$b_{w,ef}$	-	effective cross-section width of the web, mm
b_w	-	initial cross-section width of the web, mm
$d_{char,n,w}$	-	notional charring depth for the web, mm

4.2.4 Strength parameters

For simplification, this calculation method only takes into account the tension and compression stresses in the flanges. There are two possibilities for load division: a tension flange on the fire-exposed side or a compression flange on the fire-exposed side.

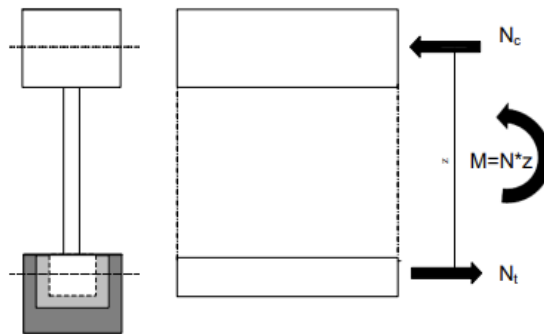


Figure 4.2.4-1 Bending moment M divided into tension (N_t) and compression (N_c) forces [3]

4.3 Formulas for calculating walls

The calculation method for walls is similar to floors, with the difference of calculating the thickness of the zero-strength layer d_0 , which has its own formula.

4.3.1 Zero-strength layer thickness d_0

Formulas for flanges on the fire exposed side in compression should be used for calculating walls. It is differentiated by the protection level of the insulation material. When calculating void cavities, it is recommended to use formulas that are specific to insulation PL2. Adhesives used in the finger joints do not have an impact on the values of compression members.

$$d_0 = \max \begin{cases} \frac{t_{f,pr}}{60} d_{char,n,1} - \frac{t_{f,pr}}{1800} d_{char,n,1}^2 + 3,8 \ln(b_f) - 4 & \text{for assemblies with} \\ & \text{PL1} \end{cases} \quad (\text{I.31})$$

$$d_0 = \max \begin{cases} \frac{t_{f,pr}}{65} d_{char,n,1} - \frac{t_{f,pr}}{2100} d_{char,n,1}^2 + 3,5 \ln(b_f) - 3,4 & \text{for assemblies with} \\ & \text{PL2 or void cavities} \end{cases} \quad (\text{I.35})$$

If the fire exposure time t is less than the failure time of the fire protection system $t_{f,pr}$ then the fire exposure time t should be used.

4.3.2 Stiffness and wall buckling

For calculating walls this proposed design model considers only compression stresses in flanges for simplification. The model assumes that the load is divided onto flanges. Load distribution considers the relation between remaining effective cross-sections of the flanges and the eccentricity of load applied. [7]

There are 3 different cases considering buckling in the wall plane:

- Case 1 - Both flanges are braced
- Case 2 - Both flanges are not braced, *this is not described in this thesis*
- Case 3 - Flange on the unexposed side is braced while the flange on the fire exposed side is not (cladding has fallen off)

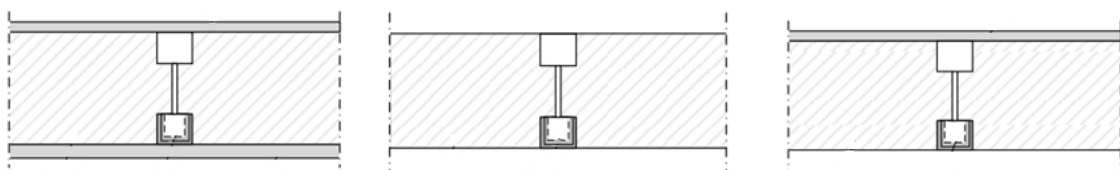


Figure 4.3.2 Case 1, Case 2, Case 3

4.3.3 Buckling out of walls plane (around y-axle)

When analyzing compression members for out-of-plane buckling, it is recommended to follow the calculation method provided in EN 1995-1-1, taking into account the effective cross-section. [5] Dimensions of the web are reduced on the used material. The method

for calculating out-of-plane buckling is the same for both Case 1 and Case 3. Buckling length is taken as I-joist length.

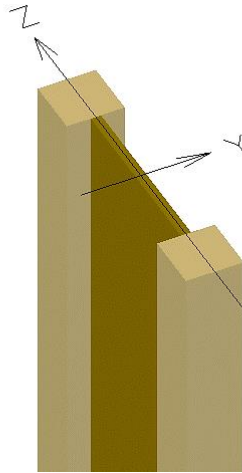


Figure 4.3.3-1 Axis for the I-joist for calculations

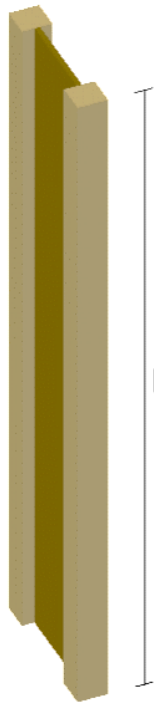


Figure 4.3.3-2 Buckling length for calculating buckling out of walls plane

4.3.4 Buckling in walls plane, around z-axle

In Case 1, the calculation should be performed following the method in EN 1995-1-1, using the parameters of the weak direction. Buckling length should be taken as the length between fasteners which is usually between 200-600 mm.

When calculating wall buckling for Case 3, the formulas used differ from those in EN 1995-1-1. However, the overall calculation process remains the same, and it is important to use the effective cross-section for the unbraced flange. Slenderness of the flange is calculated as

$$\lambda_{z,fi} = \frac{k_w L_{z,ef}}{i_z} \quad (\text{I.39})$$

with

$$k_w = 0,4 - 7 * 10^{-8} k \geq 0,1 \quad (\text{I.40})$$

$$k = 3 \frac{E_{web} I_{web,ef}}{h_w^3} \quad (\text{I.41})$$

$$h_w = h - 2h_f \quad (\text{I.42})$$

$$I_{web,ef} = \frac{L_z b_{w,ef}^3}{12} \quad (\text{I.43})$$

- where
- k - web stiffness, N/mm
 - k_w - factor for reduction of buckling length
 - $I_{web,ef}$ - moment of inertia of the web, mm⁴
 - $b_{w,ef}$ - effective thickness of the web, mm
 - h - initial cross-section height of the I-joist, mm
 - h_w - height of the web, mm
 - h_f - initial height of the flange, mm
 - E_{web} - modulus of elasticity of the web, N/mm²
 - $L_{z,ef}$ - buckling length of the I-joist in walls plane, mm



Figure 4.3.4-1 Buckling in walls plane for Case 3 [1]

4.3.5 Strength parameters

In wall structures, it is common for both flanges of I-joists to be subjected to compression loads. The load distribution between flanges should consider the relation between the remaining effective cross-sections of flanges and the eccentricity of load that is applied on the I-joist. [1]

The protection system on both sides of the I-joist prevents buckling in the wall plane. If the cladding falls off during a fire, the flange on the fire exposed side is unbraced. This increases the buckling length, but the web of the I-joist still provides some stiffness. [1]

In this situation it is necessary to distribute the load between the flanges. Loads on both flanges can be calculated according to the Figure 4.3.5-1.

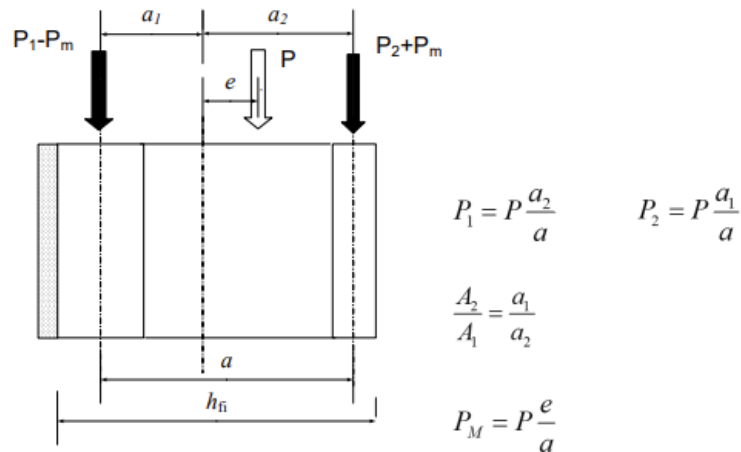


Figure 4.3.5-1 Division of loads between flanges

- where
- a - distance between the flanges centers of remaining cross-section, mm
 - a_1 - distance between the initial center of the initial cross-section and center of the flange on the unexposed side, mm
 - a_2 - distance between the initial center of the initial cross-section and center of the flange on the fire exposed side, mm
 - e - eccentricity, mm
 - P_1 - load on the flange on the unexposed side, kN
 - P_2 - load on the flange on the fire exposed side, kN
 - P_m - load from the eccentricity, kN
 - h_{fi} - remaining cross-section height, mm

5. FIRE TESTS

The tests analyzed in this thesis were previously conducted by RISE Fire Research in Norway, at the request of Masonite Beams AB. This chapter presents a description of the tests, based on the Fire test of loadbearing wooden joist construction, EN 1365-2:2014 [8], and the Fire test of loadbearing wall, EN 1365-1:2012 [9].

5.1 Full-scale floor test

The tests were carried out to evaluate the fire resistance of a loadbearing wooden joist construction, with a clear span of 4,3 m. It was performed according to EN 1365-2:2014. [8]

The loadbearing wooden joist construction contained I-shaped beams, with a height ranging from 200-300 mm and a distance between 400-600 mm. The flanges of the beams had a width of 45-47 mm and a height of 36-47 mm and were made of sawn wood with a strength class of C18 to C30, or Laminated Veneer Lumber (LVL) with parameters as shown in Table 5.1-1. The webs of the beams were constructed using 9,2-10,3 mm thick OSB or OSB3. The parameters for OSB3 can be found in Table 5.1-2 below.

Table 5.1-1 LVL parameters from the tests

Property (N/mm ²)		Joist
Bending strength	$f_{m,k}$	48
Tension strength parallel to grain	$f_{t,0,k}$	35
Compression strength parallel to grain	$f_{c,0,k}$	35
5th percentile modulus of elasticity parallel to grain	$E_{0,k}$	11600
Mean modulus of elasticity parallel to grain	$E_{0,mean}$	13800

Table 5.1-2 Properties of OSB3 according to EN 300

OSB3 Property	Test method	Unit	Board thickness range, mm	
			6 to 10	>10 to <18
Bending strength, major axis	EN 310	N/mm ²	22	20
Bending strength, minor axis	EN 310	N/mm ²	11	10
Modulus of elasticity, major axis	EN 310	N/mm ²	3500	3500
Modulus of elasticity, minor axis	EN 310	N/mm ²	1400	1400

To assemble the construction, each I-beam was secured to an edge beam using screws 5,0 x 70 mm, inserted into both flanges. The cavities between the beams were either left empty or filled with loose-fill or glass wool insulation.

At the top of the joist construction, OSB plates 18 mm were attached to the joists using screws 4,2 x 45 mm, with a distance of 200 mm. The fire exposed side of the test specimen was covered with gypsum board type A or F, with a thickness of 12,5 or 15 mm with staggered joints. These boards were secured to the joists using screws 3,5 x 38 mm.

A point loading system was used to apply a load of 1,0 kN/m², achieved by placing concrete weights and angle iron weights on the construction. The weights were applied more than 15 minutes before the fire test began. Two concrete weights and two angle irons placed above each I-beam. The test was conducted in accordance with EN 1365-2:2014.

The fire test was performed inside a gas-heated horizontal furnace. The furnace had inner dimensions of 3080 mm x 4060 mm x 1500 mm (W x L x H). The temperature inside the furnace was monitored using eight plate thermocouples, with the guidelines set out in EN 1363-1:2012.

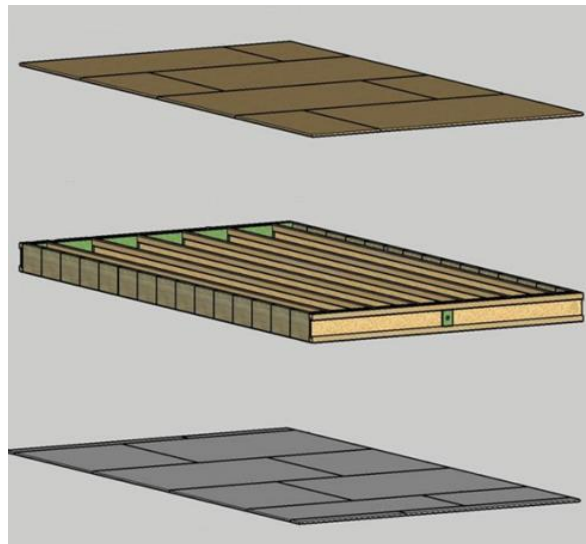


Figure 5.1-1 Timber frame assembly used in tests

After the test the point loads were removed, and the test specimen was lifted off from the furnace. The test specimen was then extinguished with water. Most of the plasterboards on the exposed side had fallen off the test specimen, apart from some areas around the edges. The underside of the OSB-plates was charred. There was burn through the web of most of the joists.

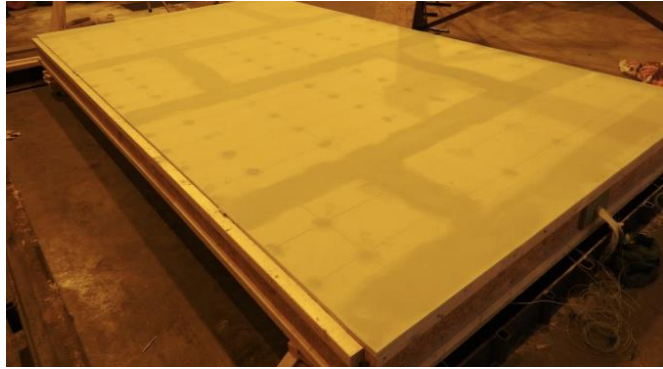


Figure 5.1-2 The exposed side of the joist construction showing the plasterboards prior to the installation of the test specimen in the test frame [8]



Figure 5.1-3 Exposed side of the test specimen after it was extinguished with water and cooled down [8]

5.2 Full-scale wall test

A fire resistance test was conducted on loadbearing timber frame wall assemblies, with a height of 3 m. The test was performed according to EN 1363-1:2012. [9]

The construction contained five I-shaped studs, with a height ranging from 160-250 mm. The flanges of the studs had width of 47-70 mm and heights of 39-47 mm and were made of sawn wood with a strength class of C18 or C30, or LVL with parameters as shown in Table 5.2-1. The I-studs webs were made of 6,7-10 mm OSB, OSB3, or wooden fiber board. The specifications for OSB3 can be seen in Table 5.1-2 on page 39 and for wooden fiber board in Table 5.2-2 on page 42.

Table 5.2-1 LVL properties used in tests

Property (N/mm ²)		Stud
Bending strength	$f_{m,k}$	32
Tension strength parallel to grain	$f_{t,0,k}$	22
Compression strength parallel to grain	$f_{c,0,k}$	22
5th percentile modulus of elasticity parallel to grain	$E_{0,k}$	8000
Mean modulus of elasticity parallel to grain	$E_{0,mean}$	9600

Table 5.2-2 Properties of wooden fibre boards used in tests [10]

HB.HLA1 Property	Test method	Unit	Board thickness range, mm	
			>3,5 to 5,5	>5,5
Bending strength, $f_{m,k}$	EN 622-2	N/mm ²	35	32
Tensile strength, $f_{t,k}$	EN 622-2	N/mm ²	26	23
Compression strength, $f_{c,k}$	EN 622-2	N/mm ²	27	24
Mean modulus of elasticity, E_{mean}	EN 622-2	N/mm ²	4800	4600

The cavities between the studs were filled with wooden fiber batt, glass wool or stone wool insulation.

At the top of the wall construction, gypsum boards were attached to the studs using screws 3,9 x 57 mm, with a distance of 200 mm on the edges and 300 mm at the center of the boards. The fire exposed side of the test specimen was covered with gypsum board type A or F, with a thickness of 12,5 or 15 mm on 34 x 95 mm laths with 3,9 x 57 mm screws with span of 200 mm at the joints and 300 mm at the center of the boards. The joints of the gypsum boards on the fire exposed side were taped with paper joint tape and then spackled.

The wall construction was mounted in a test frame with a loading equipment that applies the axial load vertically. The vertical edges of the test specimen were not restrained to the test frame and had the freedom of movement. As requested by the sponsor, a load equivalent to 250 kN was evenly distributed on the five loadbearing studs, corresponding to 50 kN/stud. The loading was applied more than 15 minutes prior to the start of the fire test.

The fire test was performed inside a gas-heated vertical furnace. The furnace had inner dimensions of 3060 mm x 3060 mm x 1200 mm (W x H x D). The temperature inside the furnace was monitored using nine plate thermocouples, with the guidelines set out in EN 1363-1:2012.

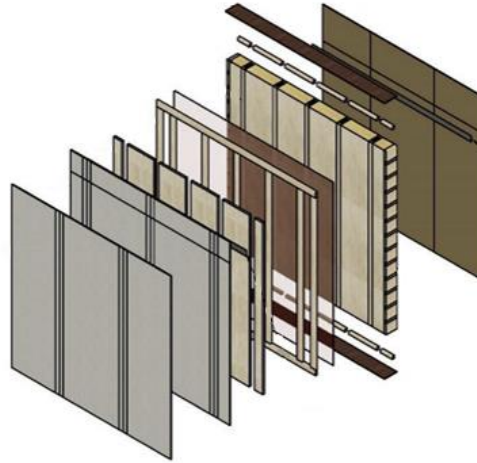


Figure 5.2-1 Timber frame assembly used in tests

After the test, the loading of the test specimen was removed, and the test specimen was lifted off the furnace and cooled with water. Most of the plasterboards on the exposed side had fallen off the test specimen, there was a clear opening into the furnace.

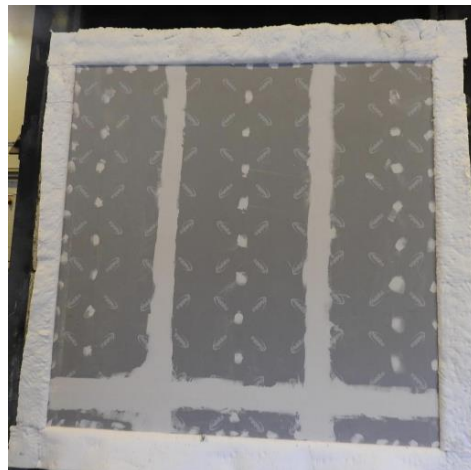


Figure 5.2-2 Exposed side of test specimen before the fire exposure [9]



Figure 5.2-3 Buckling in walls plane after the fire exposure [9]



Figure 5.2-4 Buckling out of walls plane after the fire exposure

6. COMPARISON OF TEST RESULTS AND CALCULATIONS (EN 1995-1-2:2025)

In this chapter, an analysis is presented for floors and walls, which includes a comparison of the failure times of the protection system t_f and load-bearing capacities. Test results are compared to the calculation method described in Chapter 4.

To perform the required calculations, the author created Excel tables based on the guidelines provided in Eurocode 5 Part 1-2:2025. However, the calculation method does not contain specific coefficients for void cavities. Therefore, void cavities are considered as insulation with a Protection Level 2 category in Excel tables to enable the analysis of the results.

Two calculation methods were used: one based on the failure time (t_f) from the tests, which resulted in an exposure time for the I-joist after the protection system failed; and the other based on the parameters obtained from the tests, such as the cross-section dimensions and the layers of the protection system.

6.1 Floors

6.1.1 Comparison between failure times t_f

The analysis is conducted using timber frame assemblies with void cavities or filled with insulation that met the characteristics required for Protection Level 2. Conclusions for stone wool insulation could not be done as there were not sufficient data among the test results analysed in this thesis.

18 full-scale floor tests were analyzed. The respective results are marked with 1F to 18F. Out of all the tests that were conducted, only four of them (shown in Figure 6.1.1-1 with values on page 46) resulted the gypsum board failure time t_f earlier than expected in the calculations, although this occurrence is uncommon. According to the study "The fire protection of timber members using gypsum boards" in 2022, the failure can be attributed to various factors, for example, insufficient spacing and anchorage length of fasteners, spacing of joists, type and thickness of the protection system, orientation of the assembly (wall or floor) and the type of backing material used. [6]

Failure time of gypsum cladding (t_f) in fire tests is typically registered as the time when the first significant piece of gypsum board falls off. However, this may result in longer fire exposure times, as not all of the gypsum board falls off at once.

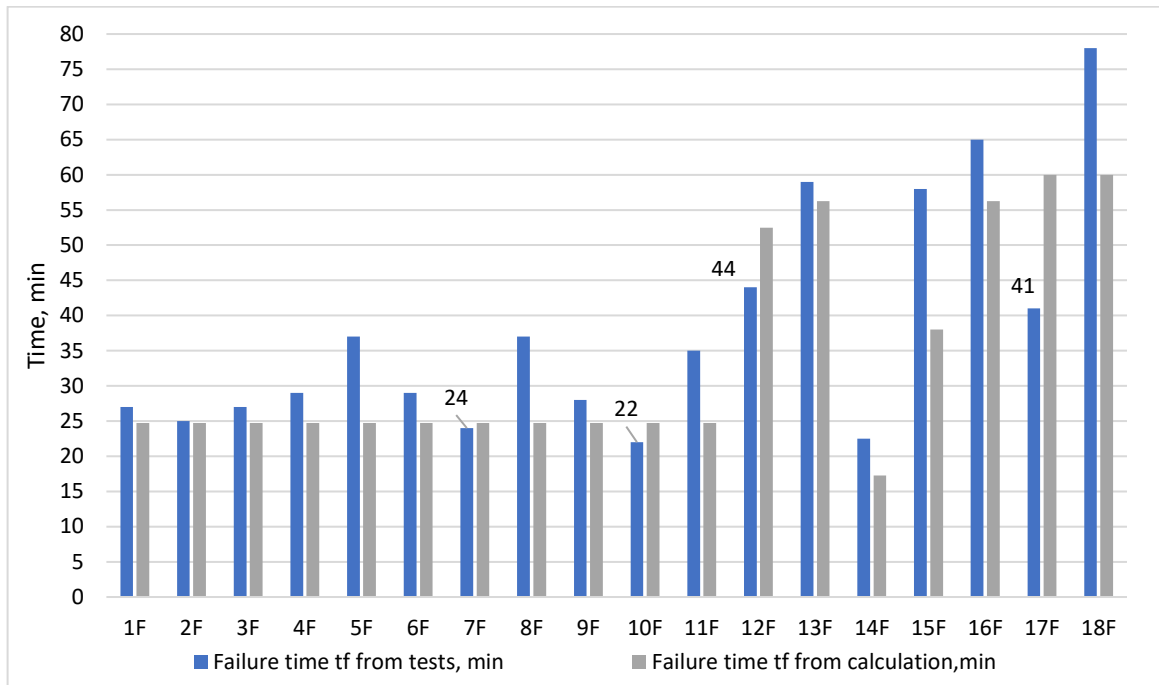


Figure 6.1.1-1 Comparison between failure times according to tests and calculation

The tests from 1F to 11F were carried out on a void cavity using type A gypsum board 15 mm on the fire exposed side. The calculated failure time of the protection system is 24,75 minutes. Out of all the tests that were carried out using void cavity, the measured value of t_f exceeded the calculated value in 72 percent of cases. These findings suggest that the calculation method is conservative and in on the safe side.

Tests 12F to 14F involved various protective layer configurations, with wood fibre batt insulation of Protection Level 2 filling the cavity. Table 6.1.1-1 lists protective layers and failure times used for each test.

Table 6.1.1-1 Protection systems and failure times

Test nr	Protection system	Failure time t_f , according to tests, in min	Failure time t_f , according to calculation, in min
12F	2x Gypsum Board type F 12,5mm (2GtF12,5)	44	52,5
13F	Gypsum board type F 15 mm + Gypsum board type F 12,5mm (GtF15 + GtF12,5)	59	56,25
14F	Gypsum board type A 12,5mm (GtA12,5)	22,5	17,25

The first mentioned layer is on the fire exposed side

Table 6.1.1-1 and Figure 6.1.1-1 on page 46 reveal that the failure time of test 12F was lower than the calculated value. This could potentially be result to poor gypsum board quality or insufficient fastening, as mentioned previously. It should be noted that, on average, the tests resulted in a 6,4% increase in failure times.

Tests 15F to 18F were performed as partially filled cavity tests. Timber frame assemblies were insulated with 100 mm glass wool. The tests included three different protection system combinations, provided in Table 6.1.1-2.

Table 6.1.1-2 Failure times

Test nr	Protection system	Failure time t_f , according to tests, in min	Failure time t_f , according to calculation, in min
15F	2x Gypsum Board type A 15mm (2GtA15)	58	38
16F	Gypsum board type F 15 mm + Gypsum board type F 12,5mm (GtF15 + GtF12,5)	65	56,25
17F	2x Gypsum Board type F 15mm (2GtF15)	41	60
18F	2x Gypsum Board type F 15mm (2GtF15)	78	60

The first mentioned layer is on the fire exposed side

Figure 6.1.1-1 on page 46 illustrates a 17% increase in the failure times from the tests. Furthermore, as seen before, there was a test where the protection system did not perform optimally. Tests 17F and 18F were both conducted using 2 layers of gypsum board type F 15mm on the fire exposed side. Comparing the failure times according to tests, the difference between those of two tests was 37 minutes, which indicates the possibility of human error on test specimens or poor quality of the protection system.

In conclusion, the test data shows that there was an approximate 16% increase in the failure times of the protection system, indicating that the calculation is reliable. Moreover, the protection system failed earlier in only 22% of the tests, which is a relatively small percentage. As shown in tests, timber frame assemblies with void cavities had better results on protective system failures than filled cavities. This is because air-filled void cavity can dissipate heat away from the plasterboard.

6.1.2 Load bearing capacity

The tests were conducted until the I-joint could no longer support any additional weight, which is referred to maximum time of fire exposure. In general, failure of an I-joint occurs when the flange on the side exposed to fire is burnt, resulting in a bottom flange's inability to resist tensile forces.

Tests 1F to 11F were conducted as a void cavity with gypsum board type A 15 mm on the fire exposed side. The parameters of the I-beams used in these tests are provided in Table 6.1.2-1.

Table 6.1.2-1 I-beam parameters from tests

Test nr	I-joist height, mm	Flange, mm (Width x height)	Flange material	Web, mm	Web material
1F	220	47x47	C30	10	OSB
2F	220	47x47	C30	10	OSB
3F	220	47x47	C30	10	OSB
4F	240	45x36	LVL	10	OSB3
5F	220	47x44	C24	9,5	OSB3
6F	240	45x36	LVL	10	OSB3
7F	220	45x36	LVL	10	OSB
8F	235	47x45	C24	9,2	OSB
9F	220	45x36	LVL	9	OSB3
10F	240	45x36	LVL	10,2	OSB3
11F	235	47x45	C24	9,2	OSB

In Figure 6.1.2-1 on page 49, the bending capacity failure occurs earlier in the design method of Annex I where t_f was taken from the test, with a difference of approximately 7,7%. During the tests, the I-joists were able to bear line load for a duration of 33 minutes in a fire situation, while the Annex I calculation method (t_f value from the test) estimated the I-joists could bear the load for about 30 minutes. The design method of Annex I (t_f calculated) gave approximately 27,2 minutes until I-joist failure, with the difference resulting from the material and measurements of the I-beams used. However, specimens with higher flanges resulted in better fire exposure times, with a 30 seconds variety.

The graph illustrates that tests 5F, 8F and 11F resulted higher fire exposure times according to tests and design method of Annex I (t_f from tests). The reason for that is the fact that the fall off time value was taken from the tests, and the calculation depended on that. The cross-section measurements did not have an effect on the bearing capacity.

To follow the dark column on Figure 6.1.2-1, it shows that the design method of Annex I (t_f calculated) remains mostly the same. The small changes come from the fact that the cross-section measurements and materials vary throughout the tests.

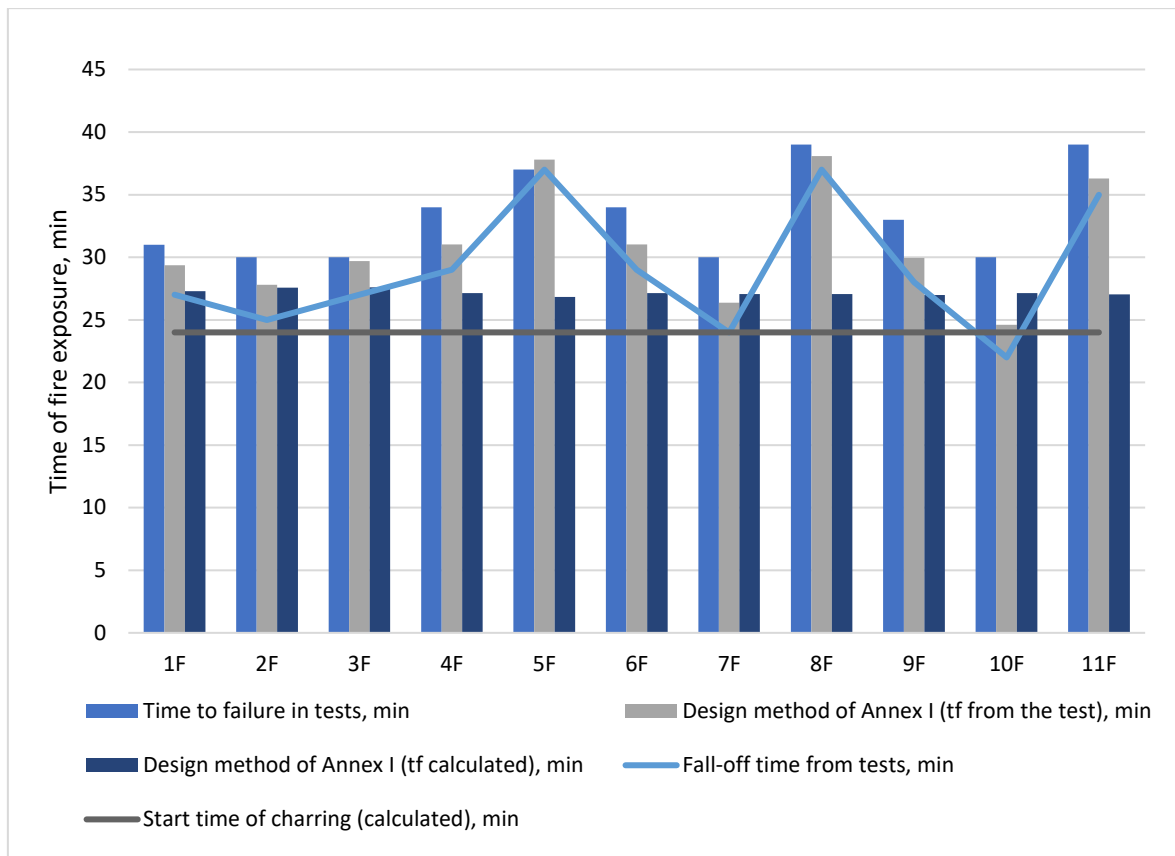


Figure 6.1.2-1 Maximum fire exposure time in tests and in calculation

Once the protection system fails, it takes about 4,3 minutes in tests for the bending strength of the I-joist to be lost. However, according to the calculation method using t_f from tests, the time from the failure of the gypsum board to I-joist failure is 1,9 minutes. Annex I calculated failure time is 2,5 minutes until I-joist failure. This means that the flange on the fire-exposed side burns completely in about 2 minutes and 30 seconds. There is a difference of about 1,75 times between the calculation and test results.

The time of charring t_{ch} has an impact on the results of the analysis. Start time of charring values are in Figure 6.1.2-1 with the dark line. It is shown that charring begins before the gypsum board falls off, which means that the cross-section starts to char before the failure time t_f . For void cavities the start time of charring t_{ch} behind the protection system (GtF 15 mm) is 24 minutes while the failure time t_f according to calculation is 24,75 minutes. According to EN 1995-1-1:2025, the values of t_f for timber frame assemblies with void cavities may be increased by 10%, which is done in this calculation.

The figure 6.1.2-1 shows discrepancy on tests 2F, 7F and 10F. This occurs because the failure of the gypsum board happens earlier than expected. Resulting in start time of charring and failure of the gypsum board happening closely the same time.

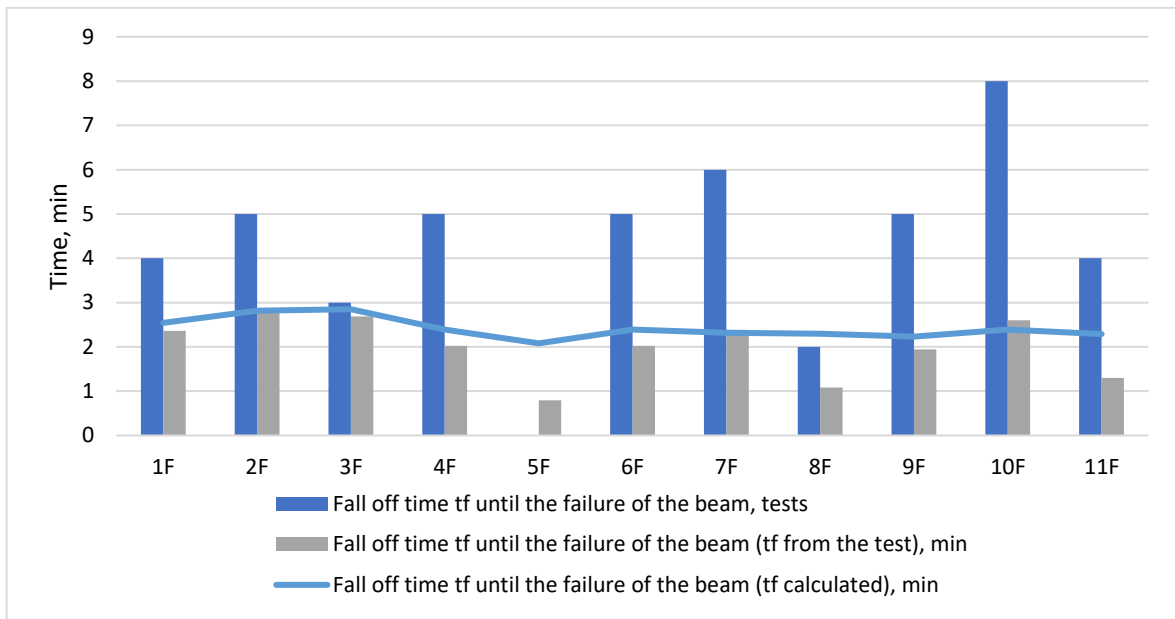


Figure 6.1.2-2 Fire duration according to tests and calculations

Figure 6.1.2-2 illustrates that calculated version according to Annex I (t_f calculated) resulted in longer fire exposure times after the failure time compared to the calculation method that used the t_f values from the tests. This is because the design method of Annex I (t_f calculated) used the start time of charring t_{ch} in accordance with the failure time, which led to a longer fire exposure time after the gypsum board failure. As a result, the cross-section of the I-joint was less charred after the fall off time of the protection system.

Test result for 5W is not visible in Figure 6.1.2-2 because the I-joint failure occurred right after the protection system failed. This is a relatively uncommon occurrence for test specimens to fail before the failure in calculations.

The author's conclusion is that in situations where void cavities are present, the difference in flange height measures for I-joists does not result in significant improvements. The most important factor for using I-shaped members is effective protection against fire.

Tests 12F to 14F involved wood fibre batt insulation in the cavities of a timber frame assembly. The tests were conducted with three different protection systems, as presented in Table 6.1.1-1 on page 46. The parameters of the test specimens are listed in Table 6.1.2-2.

Table 6.1.2-2 I-joist parameters

Test nr	I-joist height, mm	Flange, mm (Width x height)	Flange material	Web, mm	Web material
12F	250	47x47	C30	10,3	OSB
13F	200	47x47	C30	10	OSB
14F	200	47x47	C30	10	OSB

As shown in Figure 6.1.2-3 on the following page, the fire resistance time of the test specimens is dependent on the type of protection system used. Efficient protective layers can increase the fire exposure time before the test specimen fails. The difference between design method of Annex (t_f used from the tests) and test results is approximately 22%.

To compare the Annex I method (t_f calculated) and the fire test results, it was found that there is a 12% difference in the first two tests (12F and 13F), while the difference in the 14F test is approximately 42%. This difference can be attributed to the type of protection system used and the fact, that t_f according to tests is registered when the first big piece of the board falls off. Test 14F was conducted with only one layer of gypsum board type A on the fire exposed side, which may have contributed to the larger difference in fire exposure time. It is important to note that even small differences in fire exposure time can have significant effect for the structural integrity of the I-joists.

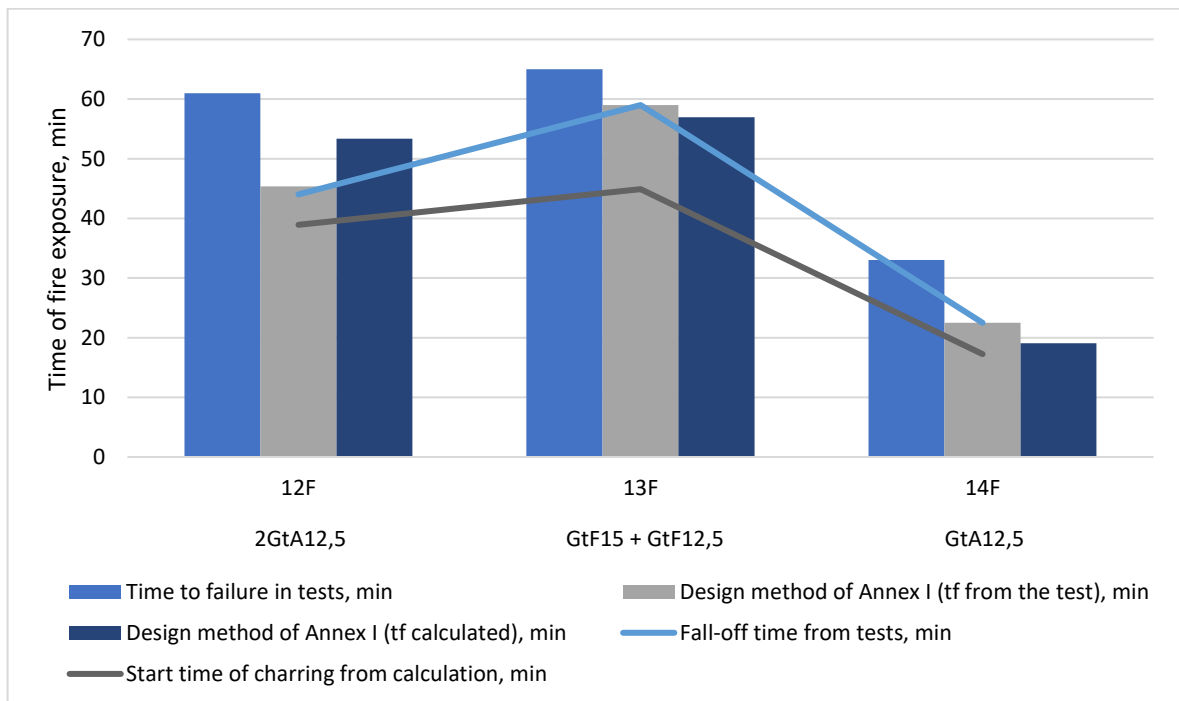


Figure 6.1.2-3 Maximum fire exposure time in tests and in calculation

Figure 6.1.2-3 shows that according to both calculation variations, specimens 13F and 14F failed before the failure time of the protection system in calculations. It is shown in the graph that the charring process had started a significant amount of time before the failure of the cladding occurred. Phase 2 off the charring process lasted about 8 minutes. As a result, by the time the protection system failed, the bottom flange of the I-joist was already completely charred and unable to take on tensile forces.

Tests 15F to 18F involved partially filled cavities, where the insulation material had greater thickness than the height of the flange on the fire-exposed side. This ensured that the lateral side of the flange was protected in fire situations. To provide protection for the I-beams, different combinations of gypsum board were used to protect test objects. More detailed description can be found on the page 47 in Table 6.1.1-2.

I-joist parameters used in tests 15F to 18F are shown in Table 6.1.2-3.

Table 6.1.2-3 I-beam parameters

Test nr	I-joist height, mm	Flange, mm (Width x height)	Flange material	Web, mm	Web material
15F	240	47x47	C18	10	OSB
16F	300	47x47	C30	10	OSB
17F	240	45x36	LVL	10	OSB
18F	235	47x45	C24	9,2	OSB

Analyzing these test results, it became evident that the bearing capacity was reached earlier according to the calculations, than the fall off of the gypsum board in tests (except test 17F). This results that the cross-section was heated or charring has started prior to the protection system failure. Ultimately this led to complete charring of the bottom flange. Maximum fire exposure time differed by approximately 27%, indicating a significant difference in calculation methods. Figure 6.1.2-4 provides further details.

Test 17F was unique in that the cladding failure time t_f occurred much earlier during the test than in calculation, see Figure 6.1.1-1 on page 46. This means that the bottom flange had less time to become severely charred before the protection system failed. As a result, the test specimen was able to withstand the fire exposure even after the protection system had failed. The method provided in Annex I (t_f calculated) resulted much longer fire exposure times because fall off time t_f was in accordance with start time of charring t_{ch} .

The author believes that test 16F provided the most accurate results since the failure time of the I-joist was relatively similar to calculation method. This means that the maximum time of fire exposure could also be the appropriate.

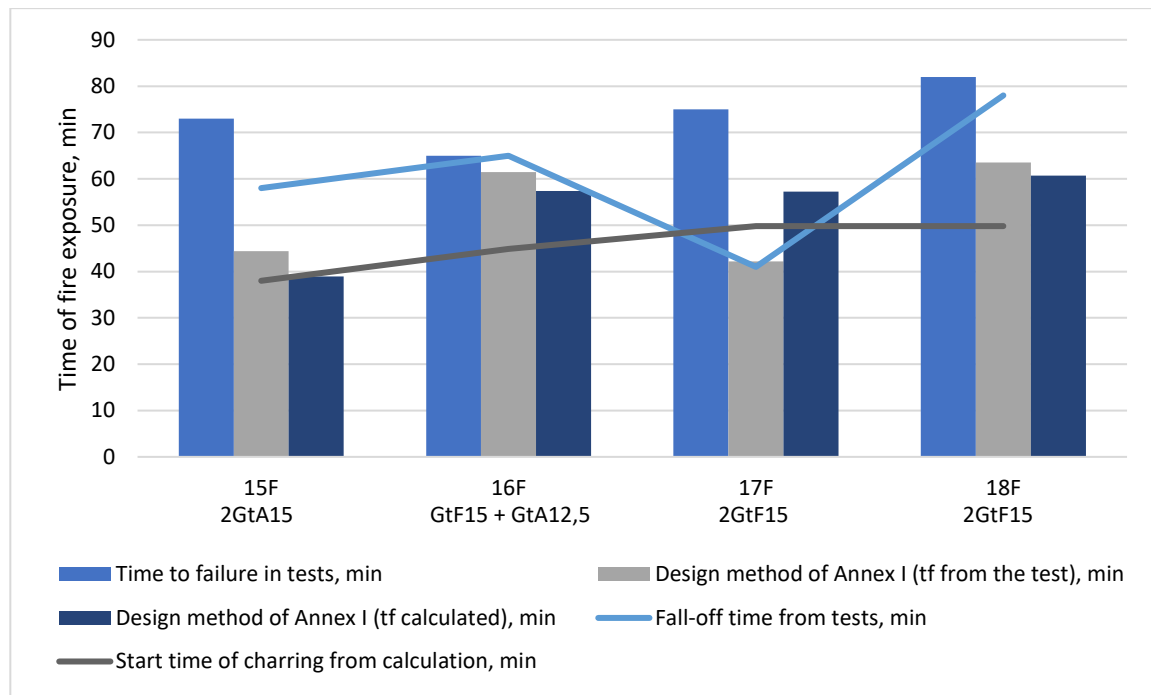


Figure 6.1.2-4 Maximum fire exposure time in tests and in calculation

The Figure 6.1.2-4 with a dark line, shows start time of charring in calculations, which explains well, why the cross-section failed before the failure time of the gypsum board.

In conclusion it is safe to conclude that the calculation method provides conservative results. By using the formulas to calculate the start time of charring, the *Chapter 4.1.2 Duration of the charring phases*, enables to determine beginning of the charring. This may explain why the calculation method result relatively short fire exposure times. The fall-off times observed in the tests were considerably higher, indicating that in reality the I-joists could endure longer fire exposure times without collapsing.

6.2 Walls

6.2.1 Comparison between failure times t_f

The analysis was conducted using 11 full-scale wall tests. The respective results are marked with 1W to 11W. The calculation of fall-off time t_f values incorporated the formulas specifically designed for walls. These formulas take into account the orientation of the walls, resulting in the gypsum board remaining intact for longer durations.

It is important to note that during testing, the t_f value is recorded when the larger portion of the gypsum board falls off, which does not necessarily indicate the complete

failure of the board. However, in the calculation process, it is assumed that when the t_f value is reached, the entire protective system will fail, leading to some inconsistencies between the calculation method and the actual test results.

The analysis involved using fully insulated timber frame assemblies. Three types of insulation were used: wood fibre batt insulation and glass wool for Protection Level 2, and stone wool for Protection Level 1. However, due to a lack of sufficient data from the test results, conclusions regarding void cavities could not be done.

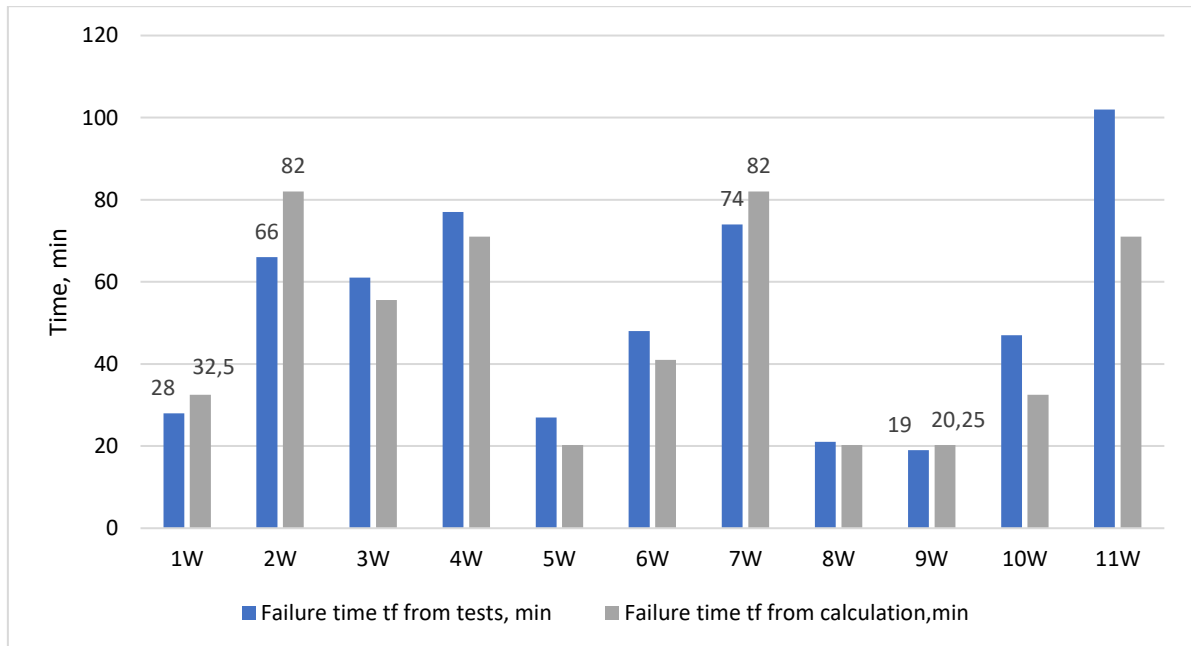


Figure 6.2.1-1 Comparison between failure times according to tests and calculation

As shown in Figure 6.2.1-1, four test specimens displayed different behavior compared to the typical scenario (marked in graph with values). In general, the calculated value t_f is lower in calculation than the actual test result. However, this difference may be attributed to factors such as a faulty fastening system, poor quality of the gypsum board, or human error in making the test specimen. Despite these disparities, the test results generally align well with the calculated values, suggesting that the calculation method may be accurate.

The author speculates that due to I-studs slender nature, they may not effectively hold gypsum boards. When the I-stud bears load, it is possible that the flanges might deform leading to an earlier fall off of the protection system. This could potentially explain why four of the tests did not present results that were expected.

Tests 1W to 7W were performed with loose fill insulation. Table 6.2.1-1 lists the various protective layer combinations in these tests.

Table 6.2.1-1 Failure times

Test nr	Protection system	Failure time t_f , according to tests, in min	Failure time t_f , according to calculation, in min
1W	Gypsum Board type F 12,5mm (GtF12,5)	28	32,5
2W	2x Gypsum Board type F 15mm (2GtF15)	66	82
3W	Gypsum Board type F 9mm + Gypsum Board type A 15mm (GtF9 + GtA15)	61	55,6
4W	Gypsum Board type F 15mm + Gypsum Board type F 12,5mm (GtF15 + GtF12,5)	77	71
5W	Gypsum Board type A 12,5mm (GtA12,5)	27	20,25
6W	2x Gypsum Board type A 12,5mm (2GtA12,5)	48	41
7W	2x Gypsum Board type F 15mm (2GtF15)	74	82

The first mentioned layer is on the fire exposed side

Table 6.2.1-1 provides a comparison between failure times of the protection system, as determined through both testing and calculation. The results mostly indicate an increase in failure times for the tests. In three of the test results, the fall-off time value in tests were approximately 14% lower than the calculated value, which is an uncommon occurrence. This could be attributed to the reasons mentioned earlier in this chapter. Four other test results showed that the calculation method produced lower values, which is a more typical outcome. The difference between these results and the calculation method was around 17%. It is worth noting that usually gypsum boards that are attached to I-studs (vertically) tend to stay in place for longer periods of time.

Tests 8W and 9W were performed using stone wool (PL1). Due to the limited number of tests conducted using stone wool for walls, there is a lack of reliable data for analysis. These tests used gypsum board type A 12,5 mm for protection. According to calculations, the expected failure time was 20,25 minutes, while the actual failure times were 21 minutes for 8W and 19 minutes for 9W. These results demonstrate a reasonably close correspondence between the tests and the calculations, with a difference of only 5%.

Tests 10W and 11W used timber frame assemblies filled with glass wool. This insulation is categorized into group with the protective abilities for Protection Level 2. This means that the calculation is quite similar to loose fill, but the difference comes from calculating protection times t_{prot} . From the tests data, author could only use two tests for analysis. Other tests contains inadequate or missing data, that could not be used to conduct conclusions.

Table 6.2.1-2 Protection system layers and failure times

Test nr	Protection system	Failure time t_f , according to tests, in min	Failure time t_f , according to calculation, in min
10W	Gypsum Board type F 12,5mm (GtF12,5)	47	32,5
11W	Habito 12,5 mm + Gypsum Board type F 15 mm (Habito12,5 + GtF15)	102	71

The first mentioned layer is on the fire exposed side

Table 6.1.2-2 on page 51 and Figure 6.2.1-1 on page 55 illustrate that the failure times for tests 10W and 11W were approximately 30% higher than calculated values. It is worth noting that, in the calculations, the Habito gypsum board was assumed to be equivalent to gypsum board type A. However, based on the test results, the Habito board did not behave like gypsum board type A, indicating that it should not be assessed using the calculation method. It may be sensible to either use the t_f value provided by the manufacturer or evaluate the Habito board as a weaker gypsum board. This approach could provide assurance in results.

In general, the failure time for walls filled with insulation increased by approximately 17%, which is similar to the 16% increase observed for floors. This suggests that the calculation method for both walls and floors provides a reserve of approximately 16%.

6.2.2 Load bearing capacity

The Eurocode 5 Part 1-2:2006 provides formulas for calculating buckling out of walls plane for Cases 1 to 3, which takes into consideration the entire remaining cross-section. However, in EN1995-1-2:2025, the calculation method for buckling in walls plane for I-studs is different. The new formulas now incorporate the remaining flange as the main calculation component. Consequently, the tests conclude when the flange on the fire exposed side is heated or completely burnt, resulting in the failure of the I-stud.

Previous chapter provides a detailed description of the protective layers of the I-studs during the tests. The cavities were insulated with various materials, including glass wool, cellulose fibre (which is categorized as Protection Level 2), and stone wool (which is categorized as Protection Level 1).

This chapter compares the test results to the Case 1 calculation method. Initially, the calculations were performed using both Case 1 and Case 3 equations. Case 3 assumes that the gypsum board on the fire-exposed side has failed completely, meaning that the whole board is no longer intact and could not provide additional stiffness. However, the

tests conducted in this study did not show this scenario. According to the test reports, the I-studs were horizontally connected with laths, which led to increase of the stiffness. The buckling was restricted in walls plane even after the fire exposure. It is important to mention that the failure time of the gypsum board was recorded when the larger chunk of the board fell off, leaving most of the board still in place to protect the I-stud.

The author concludes that as long as the laths or gypsum board are still in place, the I-stud can still bear some weight. This is because the board and horizontal supports provide stiffness to the stud in its weaker direction, which is along the wall plane (along the y-axis).

Calculating buckling for I-studs is challenging due to their slender nature. When comparing the compression of a single flange, it becomes apparent that it cannot bear much load. Therefore, using boards on each side of the flange is necessary to allow the I-stud to bear more weight and maintain its stiffness. By using gypsum boards in timber frame assemblies, the buckling length in walls plane of the I-stud is reduced. Initially, when the boards are not in place, the buckling length for buckling in the wall plane is equal to the wall height. However, after adding the gypsum board for stiffness, the buckling length becomes the distance between the fastening screws.

Tests 1W to 7W were conducted using wood fibre batt insulation in cavities. I-stud parameters used in tests are listed in Table 6.2.2-1.

Table 6.2.2-1 I-stud parameters

Test nr	I-joist height, mm	Flange, mm (Width x height)	Flange material	Web, mm	Web material
1W	160	60 x39	LVL	6,7	HB.HLA1
2W	250	47x47	C30	10	WFB
3W	250	47x47	C18	9,8	OSB
4W	200	47x47	C18	10	OSB
5W	200	47x47	C18	10	OSB
6W	250	70x47	C30	10	OSB3
7W	250	47 x47	C30	10	OSB3

There is a correlation between the failure of the protection system and load-bearing strength during a fire. As shown in Figure 6.2.2-2, tests 2W, 4W and 7W had a longer failure time for the protective system, indicating a higher level of durability during the fire.

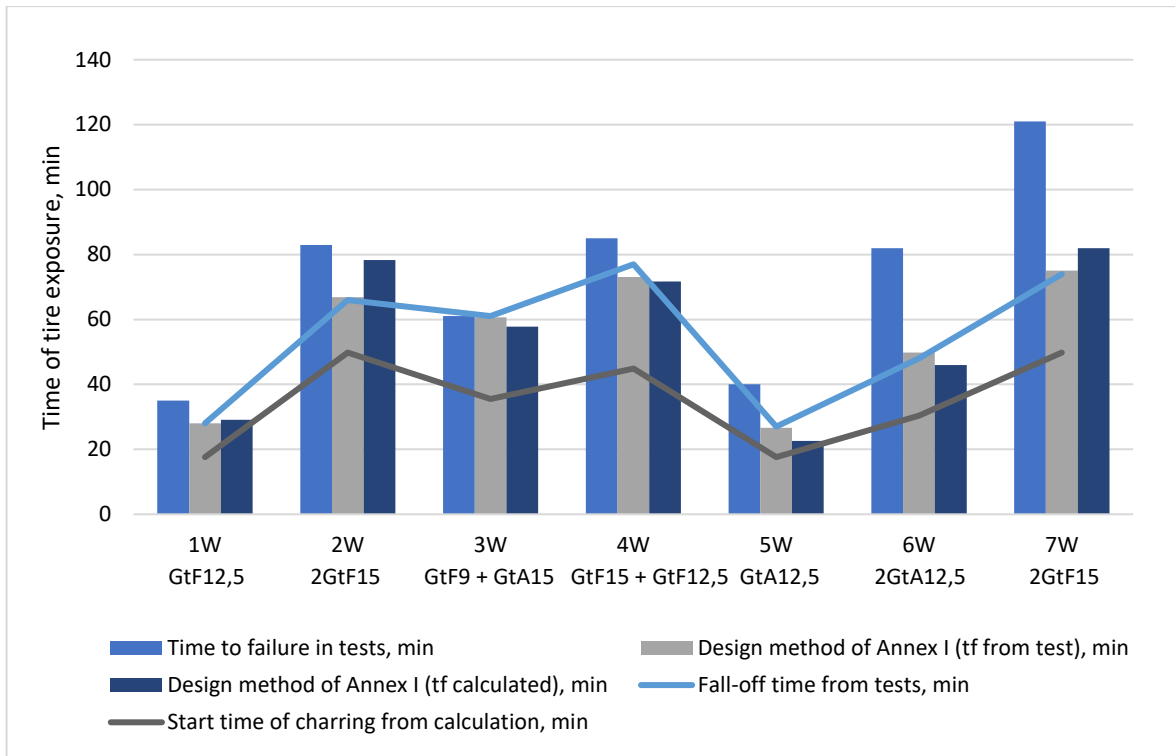


Figure 6.2.2-2 Maximum fire exposure time in tests and in calculation

Comparing the test results with the calculations, it is observed that the failure of the I-studs, according to the design method of Annex I with the fall off time (t_f) values from the tests, occurs before the fall off times of the gypsum boards. This can be attributed to the earlier start time of charring t_{ch} , as indicated by the dark line in Figure 6.2.2-2. By the time the fall off time of the gypsum board occurs, the flange on the fire-exposed side is already fully charred, leading to a loss of bearing capacity for the I-stud. It is noteworthy that the design method for Annex I (t_f calculated) (dark blue column), resulted longer fire exposure times in tests 1W, 2W and 7W compared to the results calculated with Annex I method (t_f from tests). This discrepancy can be attributed to the fact that in those specific tests, the fall of time in tests occurred earlier than in calculation method. Consequently, the Annex I method (t_f from tests) produced lower values in those cases.

Comparing the test results to the calculations, the author believes that the most accurate test was 3W, because the failure of the I-stud occurs right when the protection system fails. This means that the temperatures behind the protective layers have reached 300 degrees and charring has started before the failure time t_f .

Tests 8W and 9W were conducted using stone wool as the insulation in cavities. However, only two tests met the criteria set for this thesis, which means that the

conclusions done in this section may not be entirely accurate due to the lack of sufficient data. Table 6.2.2-2 lists the parameters for the I-studs used in both tests. Both of these tests were conducted with Gypsum board type A 12,5 mm as a protection system.

Table 6.2.2-2 I-stud parameters

Test nr	I-joist height, mm	Flange, mm (Width x height)	Flange material	Web, mm	Web material
8W	200	47x47	C30	10	OSB3
9W	200	47x47	C30	8	WFB

The results from tests 8W and 9W showed similarities, with a fall off time of approximately 20 minutes and the failure of the I-stud occurring after 57 minutes from the beginning of the fire. This means that according to tests, after the protection system fails, the studs are exposed to fire for an additional 37 minutes before failing. In comparison, the calculation methods resulted in a possible fire exposure of just 6 minutes, indicating a significant difference between the two. The two calculation methods resulted in similar fire exposure times, which may be due to the similar t_f values appeared in tests.

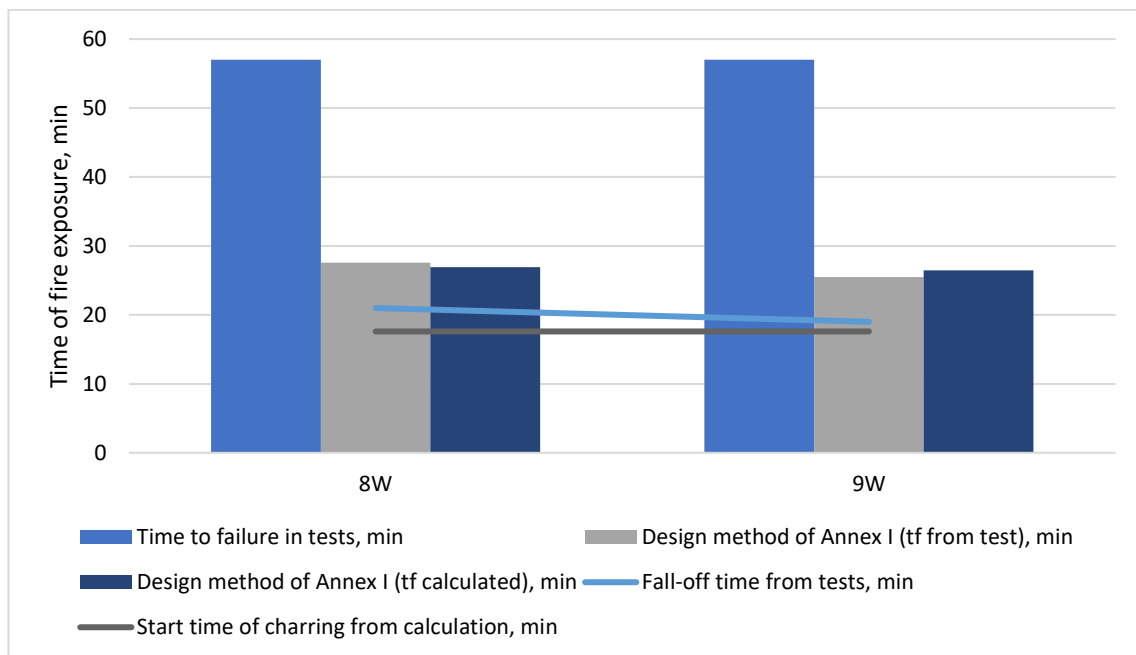


Figure 6.2.2-3 Maximum fire exposure time in tests and in calculation

Figure 6.2.2-3 shows that the failure of the I-stud, according to both calculation methods, occurs after the failure of the protection system. This could be due to the use of stone wool as the insulation material, which has better properties for fire and results in a higher level of protection (PL1). The figure also indicates that the start time (t_{ch}) of

charring was relatively short before the failure time of the protection system (t_f according to tests), resulting in a higher failure time of the I-stud. However, it should be noted that the failure time t_f was determined based on the pieces falling off from the gypsum board, which does not necessarily mean that the entire board failed and lost its integrity.

Tests 10W and 11W with glass wool were conducted using two different protection systems, for 10W it was gypsum board Type F 12,5mm and for 11W Habito 12,5 mm on the fire exposed side + gypsum board type F 15 mm as a second layer. I-stud parameters are presented in Table 6.2.2-3.

Table 6.2.2-3 I-stud parameters

Test nr	I-joist height, mm	Flange, mm (Width x height)	Flange material	Web, mm	Web material
10W	200	47x47	C18	10	OSB
11W	200 (HI)	70x47	C30	10	OSB3

As illustrated in Figure 6.2.2-4 on page 62, the I-stud failure occurred 22 minutes after the fall off time t_f in test 10W and 11 minutes after the fall off time t_f in test 11W. When using the calculation method according to design method of Annex I (with t_f from the tests), the maximum fire exposure time for I-stud decreased by approximately 40%. Comparing the values attained from two different calculation methods revealed that the results were quite similar. However, the difference between calculations and tests could be associated with the start time of charring t_{ch} , which begins much earlier in calculation. By the time the protection system falls off, the flange on the fire exposed side has already charred, resulting the I-stud incapable of bearing any further load.

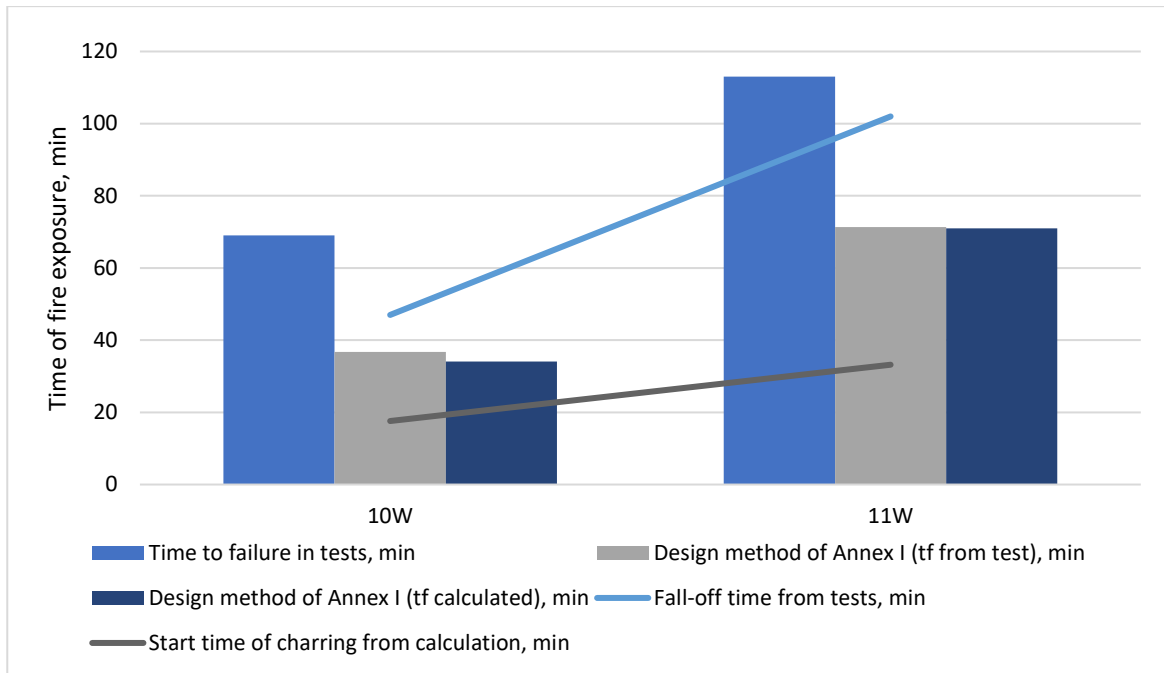


Figure 6.2.2-4 Maximum fire exposure time in tests and in calculation

Table 6.2.2-3 on the previous page indicates that the I-stud in the second test (11W) had a wider flange on the fire exposed side. This could potentially explain why the stud was able to withstand such a long time of fire exposure. Additionally, the use of Habito gypsum board in the test may have also contributed to the longer fire exposure time.

6.3 Conclusions

In conclusion, the tests indicate that effective protection is crucial in covering the I-shaped cross-sections, as this leads to higher fire exposure times and ultimately increases the bearing capacity.

The calculations for floor assemblies with void cavities provided more accurate results compared to the tests. The bearing capacity of these assemblies is dependent on the effectiveness of the fire protection system. If the lateral sides of the flange and web are not insulated, the bottom flange can burn quickly after the protection system fails. The fully calculated value for bearing capacity differed by approximately 26-27 minutes, while the value using t_f from the tests was noticeably higher at around 31 minutes. It is important to note that Phase 2 (time from t_{ch} to t_f) of the charring lasted for approximately 5 minutes.

The calculation methods used for floor assemblies filled with insulation indicate that the I-joists failure occurred before the failure of the protective layers. This suggests that

the use of insulation with a Protection Level 2 rating may not be that effective in fire scenarios. The charring process starts way before the gypsum board's fall-off time, causing the fire-exposed flange to char and leading to a loss of bearing capacity before the protection system fails. Phase 2, which is time from t_{ch} to t_f , lasted approximately 11 minutes.

To compare the failure time of the protection system for walls, the results were somewhat unexpected. Typically, the calculation method gives smaller results while the tests result in higher values. However, in these tests, the gypsum board failed in three instances before the failure in the calculation. This could be due to poor quality gypsum board or inadequate fastening. Overall, the difference between the test results and calculations was approximately 15%.

To compare bearing capacity of walls from the test results with the calculated values, it can be concluded that in most cases, the failure of the I-studs occurred earlier than the failure time of the protection system, except for cavities filled with stone wool. Using stone wool insulation provided better protection to I-studs compared to other types of insulation. The fall off time of the protection system occurred before the failure of the I-stud, indicating that using insulation with parameters from Protection Level 1 is the most effective approach.

Case 3 approach in wall buckling calculation is typically used after the fire exposure and the calculation method provides formulas to assess such scenario. However, it is important to acknowledge that this approach may not be guaranteed in every case, as the post-fire conditions are often uncertain. Through this research, it has been discovered that the Case 3 situation may not be suitable for every fire situation.

During the calculation of I-shaped cross-sections prior to the failure of the protection system, it is evident that both the strength classes of the wood and the dimensions of the cross-section play a significant role. However, in this thesis, the author did not observe any significant difference between wood classes when calculating situations after the fall-off of the fire protection system. When the latter occurs, the load bearing capacity of the I-joists will decrease rapidly. When web of the I-joist is charred, the I-joist collapses within a short time, independent of its cross-section height.

7. PROPOSITIONS FOR EUROCODE 5 PART 1-2:2025

In this chapter, the author discusses the errors that were encountered during the calculation process of various cross-section options using Excel tables. Additionally, some suggestions are presented to help simplify the calculations and avoid potential mistakes in the future.

The initial stage of the I-joist calculation process involved determining the failure times and times when the charring started. This was completed using the Separating Function Method from EN1995-1-2:2025 section 7.3. An error was identified in formula 7.61 from Table 7.1. To calculate $t_{\text{prot},0,i}$ for mineral insulation, result should be taken as minimum of the two formulas presented in that equation.

Mineral wool cavity insulation PL2	$t_{\text{prot},0,i} = 0$ for $h_i \leq 40$	(7.61)
	$t_{\text{prot},0,i} = \max \left\{ \begin{array}{l} \left(\frac{\rho_i}{1430} + 0,046 \right) \cdot h_i + 13 \\ 30 \end{array} \right.$ for $h_i > 40$	

Figure 7-1 Extracted part from Eurocode 5 Part 1-2, Table 7.1 [5]

The start time of charring of the web $t_{\text{ch},w}$ is dependent on t_{prot} calculation, which is different for I-shaped cross-sections. To achieve correct values, the layer order in calculation should follow the same order as the heat path. The calculation should be done using insulation with thickness found with formula I.30 from Annex I. The layer behind insulation should be the web of the I-joist. This approach would result in a more accurate values.

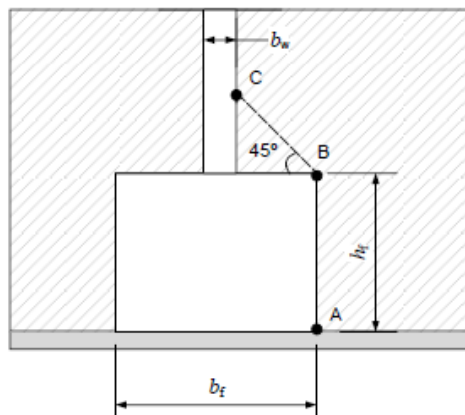


Figure 7-2 Heat paths on the lateral side [5]

Chapter 4.2.3 of this thesis outlines the formulas for calculation notional charring rates for the web. It is important to note that, as per Eurocode 5 Part 1-2:2025 (5.3.2.2

Notional design charring rate), the basic charring rate β_0 for OSB must be taken as β_n . This takes into consideration the thickness factor k_h and density factor k_ρ . Therefore, the basic design rate value in calculations should be taken according to the following formula:

$$\beta_0 = \beta_n = \prod k_i * \beta_0 = k_h * k_\rho * \beta_0 = \sqrt{\frac{20}{h_p}} * \sqrt{\frac{450}{\rho_k}} * \beta_0 = \sqrt{\frac{20}{10}} * \sqrt{\frac{450}{650}} * 0,9 = \mathbf{1,06 \text{ mm/min}} \quad (5.2)$$

In the opinion of the author, it is recommended to include this formula (5.2) in Annex I alongside the calculations that describe the web.

The factors $k_{s,n,1}, k_{s,n,2}$ used in the calculations are relevant to insulation materials and were not applicable to void cavities. However, to enable the calculations related to void cavities, the author of the thesis used factors for insulation PL2. Out of the various options for calculating the factors, it was assumed that the behavior of PL2 insulation is the most similar to void cavities.

The author noticed that the formulas for wall buckling were provided without a corresponding figure to illustrate the axial situation. Calculating buckling is already complex, given the I-stud's behavior, cross-section slenderness, and the use of different materials. Therefore, potential figures have been included below.

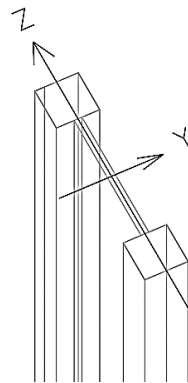


Figure 7-3 Illustration of axial situation

Calculating the times, that the charring phase is considered, has some limitations. It should be noted that the charring phase durations can not have negative values. Usually the times are calculated as

For Phase 2

$$t_{ph2} = t_f - t_{ch}$$

This approach is valid if the failure time of the protection system (t_f) occurs earlier than the fire duration (t), $t > t_f$. However, if the failure time (t_f) is greater than the time of fire exposure (t), $t_f > t$, the calculation for Phase 2 should be performed as

$$t_{ph2} = t - t_f$$

For Phase 3

$$t_{ph3} = t_a - t_f$$

This current formula is based on the situation, where the failure of the protection system occurs earlier than the fire exposure time, $t > t_f$. However, it is important to note that if the fire exposure time (t) is earlier than the failure of the protection system (t_f), the Phase 3 does not exist and the duration of the Phase 3 should be considered as 0.

For Phase 4

$$t_{ph4} = t - t_a$$

Phase 4 is relevant when the fire exposure time (t) exceeds the time of consolidation (t_a). If the fire exposure time occurs earlier than the consolidation time, the duration of Phase 4 should be considered as 0.

SUMMARY

Studies have demonstrated that utilizing wood is an effective approach for constructing sustainable buildings. By using timber, there is no compromise on performance or load-bearing capabilities. Initially, wood was often avoided as a construction material due to the lack on integrity in fire situations. However, over the years, effective methods have been developed to protect wood from fire. One way to incorporate wood in constructions is through the use of I-shaped members in timber frame assemblies.

Timber frame assemblies with I-joists can be used in roofs, walls of floors. I-shaped elements consist of flanges and a web. Due to the cross-sections slenderness and various materials, the calculation in fire situations is complex matter. The existing Eurocode does not provide calculation method for I-shaped cross-sections. However, there is a Guideline "Fire Safety in Timber Buildings" that covers the I-joists in floor assemblies. Wall and void cavity calculations are not included.

The aim of this thesis was to evaluate the calculation method for I-shaped members provided in Annex I of EN 1995-1-2:2025. The purpose was to eliminate any potential calculation errors that may occur during the design of constructions. In order to test the equations, the author created Excel tables, that calculate the I-shaped cross-sections after the fire exposure. Additionally, the Excel table also included calculation of protection times, according to the new *Eurocode 5 Part 1-2:2025 Section 7.3 Separating function method*. This enabled to possibility to evaluate those formulas as well.

Calculation results were then compared to the test results that were conducted using protection systems, such as gypsum boards and insulation. The comparison was performed using two different approaches for calculation. One of them was using failure time of the protection system from the test and continuing calculation as Annex I requested. The other approach was to calculate all the values according to the formulas and compare the results with tests and former method. As expected, the overall fire exposure time results were higher than the calculated values. The calculation methods held lower results and remained on the safe side.

The results of full-scale fire tests were as expected - the protection system of I joists plays a significant role in maintaining bearing capacity. This means, that it is crucial to use effective protection system, since the I-joists started to heat up and char even before the protection systems failure occurred.

Furthermore, there is a new approach for calculating walls in the new Eurocode 5 Part 1-2:2025, where wall buckling is categorized into three groups: Case 1, Case 2 and Case 3. In this thesis, the evaluation focused on Case 1 and 3. Initially, it was assumed that after the fire exposure, the calculation should be carried out according to formulas specified for Case 3. However, it should be noted that Case 3 expects the failure of the whole gypsum board, which is not always the case after the fire exposure. The tests examined in this thesis involved the use of horizontal laths and gypsum boards to improve the stiffness of the I-studs. Consequently, the analysis was conducted using the calculation values specified for Case 1.

In addition to above, this thesis proposes improvements to Eurocode 5 Part 1-2:2025 Annex I to simplify the calculation process and provide additional explanations and figures to better describe the calculation methodology. The author noticed faulty equations and incorrect explanations, which are presented in Chapter 7. One of the simplest and crucial addition to Annex I should be inclusion of limitations for charring phase durations. Currently, the calculation method describes these durations with the presumption that the fire exposure time exceeds all of the charring phase times. However, it is equally important to address the situations where the fire exposure time is shorter than charring phase durations. This aspect is important in the calculation process as it is one of the first steps in designing I-shaped cross-sections.

It is important to point out that current thesis analyzed a limited number of tests, which implies that final conclusions might not be reliable. Further testing is required to thoroughly evaluate the bearing capacity of I-studs and I-joists in fire situations. Furthermore, to specify the results in this thesis, the author suggests that the failure times of gypsum boards in fire situation should be to specifically evaluated when used on I-studs. The application of load on the stud may cause deformations on flanges, potentially leading to earlier detachment of the gypsum board.

KOKKUVÕTE

Puidu kasutamine hoonete konstruktsioonides on tänapäeval väga levinud. See võimaldab ehitada jätkusuutlikult ja endiselt säilitada konstruktsioonide kandevõime ning visuaali. Varasemalt on eelistatud ehitiste kandvate osade konstrueerimisel teisi materjale, pidades puidu puhul probleemiks tuleohutust. Kuid aja jooksul on välja töötatud tõhusad lahendused, mis kaitsevad puitu tule eest.

Puitu saab rakendada kasutades seda I-kujuliste elementidena seinte,- põrandate- ja katusekonstruktsioonides. Need komposiitlemendid koosnevad kahest vööst ja nende vahelisest seinast. I-ristlõiked on saledad ja koosnevad erinevatest materjalidest, mistõttu nende arvutamine nõuab keerukaid valemeid. Praegune Eurokoodeks 5 ei sisalda arvutusmeetodit I-elementide tulepüsivuse hindamiseks. Seega on ainus võimalus teostada arvutusi käsiraamatu "Tuleohutud puitmajad" abil. Kuigi arvutuseks on valeimid olemas, kehtivad need vaid soojustatud I-taladega vahelaekonstruktsioonide puhul, ehk need pole sobilikud kasutamiseks seinte ja tühimikega vahelagede olukordades.

Selle töö eesmärk oli hinnata puidust I-ristlõigete tulepüsivust uue Eurokoodeks 5 arvutusmeetodiga. Oluline oli leida valemities ebakõlad, mis võiksid tulevikus takistada I-talade ja I-postide dimensioneerimist. Arvutusmeetodi testimiseks koostas autor Exceli tabelid, mis sisaldasid ka kipsplaatide ja isolatsioonide kaitseaegade leidmist. Kaitseaegade leidmise meetodit on kirjeldatud uues Eurokoodeksis peatükis 7.3. Selle lisamine võimaldas hinnata ka nende valemite toimivust.

Arvutusmeetodi tulemusi võrreldi täismõõdus tulekatsete tulemustega, kus I-kujuliste elementide kaitsmiseks erinevaid kihte, näiteks kipsplaate ja isolatiooni. Arvutusmeetodi läbiviimiseks rakendati kahte viisi. Esimeses meetodis kasutati Lisa I valemeid, võttes tõrketekkeajaks katsest saadud tulemus. Teises lähenemises kasutati ainult arvutuslikke väärtusi. Analüüsi tulemused oli eeldustele vastavad – enamikul katsetel oli puidust I-elementide tulepüsivusajad arvutuslikest suuremad. Seega võib järeldada, et arvutusmeetod annab tagavara ning saab kasutada I-kujuliste elementide arvutamiseks tulekahjuolukorras.

Tulekatsete tulemused kinnitasid eeldust, et kaitsvate kihtide olemasolu on oluline kandevõime säilitamiseks. Kuna I-elementide puidust vööd hakkavad kuumenema ja söestuma juba enne kaitsekihtide tõrketekkeaega, on oluline puitu kaitsta otsese tule eest.

Uues Eurokoodeksis on esitatud arvutusviis, mis võimaldab hinnata seinte käitumist tulekahju olukorras. Eraldi on välja toodud valemid seinte nõtkumise arvutamiseks erinevates olukordades: Case 1, Case 2 ja Case 3. Selles töös võeti kasutusele Case 1 ja Case 3 valemid. Esialgu eeldati, et pärast tulekahjut, arvutus peaks põhinema Case 3 valemitel. Seda põhjusel, et Case 3 eeldab, et pärast tulekahju on kipsplaat täielikult hävinenud ning nõtkumist seina tasandis ei takista miski. Tegelikuses võib aga esineda olukord, kus kipsplaat ei ole tulekahju lõppedes täielikult hävinenud. Lisaks tuleb arvesse võtta, et tõrketekkeajaga on fikseeritud aeg, millal esimene suurem kipsplaadi tükk ära kukkus, mitte aeg, millal kogu kipsplaat ära kukkus. Katsed, mida selles töös analüüsiti, sisaldasid horisontaalseid puitlatte ja kipsplaati, mis suurendasid I-postide jäikust. Neist tingimustest lähtudes, võrreldi katsetulemusi arvutustega, mis põhinesid Case 1 valemitel.

Lisaks eelmainitule, pakub töö autor välja täiendused, mis võiks sisse viia uue Eurokoodeksi 5 osasse Lisa I. Nende muudatuste eesmärk on lihtsustada keerulist arvutusprotsessi ning anda selgitusi ja jooniseid, mis illustreeriksid arvutusmeetodit. Peatükis 7 on välja toodud ettepanekud, mille sisseviimist võiks kaaluda enne uue Eurokoodeksi ilmumist. Üks kõige lihtsamaid ja olulisemaid täiendusi Lisa I arvutusmeetodis oleks piirangute lisamine söestumisfaaside kestuse arvutustesse. Hetkel eeldavad valemid, et tulekahju kestus on pikem kui erinevate söestumisfaaside kestused. Tegelikult on samuti olulised olukorrad, kus tulekahju kestus ei ületa söestumisfaaside kestusi. See täiendus oleks oluline, kuna söestumisfaaside arvutamine on üks esimestesi samme I-kujuliste elementide tulepüsivuse hindamisel.

Väga oluline on märkida, et selles töös on analüüsitud vähe katsetulemusi, mis tähendab, et lõplikud järeldused võivad olla ebatäpsed. Kindlasti peaks sooritama lisakatseid, et saaks hinnata I-talade ja I-postide kandevõimet tulekahju olukorras. Täiendavat testimist vajab olukord, kus kipsplaadid on kinnitatud I-postide külge. On teada, et I-posti võöd deformeeruvad koormuse all ning on vajalik teada, kas see mõjutab ka kipsplaadi püsivust võö küljes. Lisakatsetused aitaksid täpsustada ja täiendada arvutusmeetodeid ning tagada suurem usaldusväarsus tulekindluse hindamisel.

REFERENCES

- [1] M. Beams, "The I-joist Handbook", Stockholm: Masonite Beams AB www.masonitebeams.se, 2022.
- [2] H. Manguse, „Charring analysis of wooden I-joists in standard fire", TTÜ press Tallinn, 2020.
- [3] *Fire Safety in Timber Buildings: Technical Guideline for Europe*, Stockholm: SP Technical Research Institute of Sweden, 2010.
- [4] M. Tiso, „The Contribution of Cavity Insulations to the Load-Bearing Capacity of", TTÜ press, Tallinn, 2018.
- [5] *Eurocode 5 - Design of timber structures. Part 1-2: Structural fire design : EN1995 1-2:2025 (E). Final draft.*, 2025.
- [6] N. M. A. Just, „The fire protection of timber members using gypsum boards, ResearchGate, 2022.
- [7] K. N. M. a. A. Just, "Improved fire design model for walls and floors with I-joists' Firewood, 2022.
- [8] E. D. Wormdahl, *Test report - Masonite Beams AB, Fire test of loadbearing wooden joist construction, NS-EN 1365-2:2014*, RISE Fire Research, 2018.
- [9] E. W. Jacobsen, *Test report - Masonite Beams AB, Fire test of loadbearing wall, NS EN 1365-1:2012*, RISE Fire Research, 2019.
- [10] H. Austria, „dataholz.eu," 01 June 2018. [Võrgumaterjal]. Available https://www.dataholz.eu/fileadmin/dataholz/media/baustoffe/Datenblaetter_en/hb_en_01.pdf. [Kasutatud 30 April 2023].
- [11] *Eurocode 5 - Design of timber structures. Part 1-2: Structural fire design : EVS-EN 1995-1-2:2006*, Tallinn: Estonian Centre for Standardisation, 2006.
- [12] *Eurocode 5 - Design of timber structures. Part 1-1: General - Common rules and rules for buildings : EVS-EN 1995-1-1:2006*, Tallinn: Estonian Centre for Standardisation, 2006.